ONSET TIME AND DURATION OF CORONA ACTIVITY ON VENUS: STRATIGRAPHY AND HISTORY FROM PHOTOGEOLOGIC STUDY OF STEREO IMAGES

A. T. BASILEVSKY[1,2] and J. W. HEAD[1]
[1]*Vernadsky Institute of Geochemistry and Analytical Chemistry, Moscow 117975, Russia, e-mail: abasilevsky@glasnet.ru;* [2]*Department of Geological Sciences, Brown University, Providence, RI 02912, U.S.A., e-mail: James_Head_III@Brown.edu*

(Received 23 September 1997; Accepted in final form 12 February 1998)

Abstract. The details of stratigraphic units and structures making up six coronae and their regional surroundings on Venus were examined using full resolution Magellan images and stereoscopic coverage. Altimetry and stereoscopic coverage were essential in establishing the local stratigraphic relationships and the timing of corona-related topography. The degree of preservation of signatures of earlier corona-related activities and the scale of later corona-related activities vary significantly from corona to corona. We compared the geologic sequence in each corona to regional and global stratigraphic units, placing the coronae in the broader context of the geologic history of Venus. The results of this study were compared with earlier analyses bringing the total number of corona considered to about 15% of the total corona population. We found that corona started forming soon after tessera formation and largely spanned a significant part of the subsequent geologic history of Venus, over about 200–400 million years. Topographic annulae were initiated in early post-tessera time but were largely completely formed by the time of emplacement of regional plains with wrinkle ridges. Some coronae ceased activity by this time, while others continued until closer to the present, although showing evidence of waning activity. Coronae-associated volcanism dominated many coronae during this later stage. Convincing evidence of pre-regional plains corona- related volcanism was not found in the population examined here. We conclude that coronae formed in a two stage process; the first stage (tectonic phase) involved the annular warping of early extensive stratigraphic units of volcanic origin and the second (volcanic phase) involved coronae-related lava flow activity and local fracturing. For the vast majority of coronae, the first tectonic phase was largely complete prior to the emplacement of the regional plains (Pwr, plains with wrinkle ridges). The vast majority of corona-related volcanic activity (emplacement of Pl, lobate flows) occurred subsequent to the emplacement of regional plains. We found no evidence of coronae initiation in substantially later periods of the observed history of Venus.

1. Introduction

Coronae are circular to oval volcanic-tectonic features hundreds of kilometers across; about three dozen were first found in the analysis of radar images of the northern part of Venus taken by Soviet Venera 15 and Venera 16 spacecraft (Barsukov et al., 1984, 1985, 1986; Basilevsky et al., 1986). Several attributes of coronae led to the conclusion that they are the surface expression of upwelling mantle plumes, otherwise considered as hot mantle diapirs: (1) the sizes of the features,

Earth, Moon and Planets **76:** 67–115, 1997–1998.

(2) the characteristic presence of a circular annulus standing above the surrounding plains and typically deformed by concentric faults and folds, and (3) association with volcanic flows and edifices (Barsukov et al., 1984, 1985, 1986; Basilevsky et al., 1986; Pronin and Stofan, 1988, 1990; Schubert et al., 1989; Stofan and Head, 1990; Nikishin et al., 1992). Analysis of radar images with higher spatial resolution taken by the US Magellan mission for nearly all the surface of the planet increased the number of identified coronae to about 350 (Stofan et al., 1992; Head et al., 1992). On the basis of the Magellan data, coronae were described in much more detail and this led to a more in-depth consideration of the mechanism of formation due to upwelling and subsequent relaxation of mantle plumes and the overlying lithosphere (Squyres et al., 1992; Janes et al., 1992; Sandwell and Schubert, 1992).

Later studies of coronae essentially concentrated on the detailed description of corona geology usually with analysis of the age sequence of the material units comprising them, their structures, and their relations with regional geologic units and structures (Basilevsky and Head, 1994; 1995a–c; Basilevsky, 1995; Magee and Head, 1993; Baer et al., 1994; Jackson et al., 1995; Chapman, 1996; Pronin, 1997). Theoretical modelling of their origin has also been undertaken (Koch, 1994; Janes and Squyres, 1995; Smrekar and Stofan, 1996; Smrekar and Parmentier, 1996; Musser and Squyres, 1997). However convergence between the geologic studies of coronae and detailed theoretical models of this process has not yet been completely accomplished.

This paper aims to continue the stratigraphic approach in the geologic analysis of coronae with the goal of attempting to answer the following questions which are important as constraints in working out comprehensive models of the corona formation process:

(1) When in the local, regional, and global stratigraphic context, did different coronae start to form and when did their evolution cease? Are some coronae in their initial stages of formation on Venus today?

(2) Did coronae formation occur synchronously in the sense that corona elements of the same type in different coronae formed at approximately the same time, or, was the evolution of a single corona absolutely not correlated in time with the evolution of another coronae? Have some coronae finished their life cycle, while others are in intermediate stages or just beginning?

(3) What was the absolute time duration of the life cycle of individual coronae? If coronae are not forming today, what was the time duration from the beginning of formation of the coronae population until its termination?

The specific approach of this analysis is that we studied six coronae which were imaged by Magellan (Figure 1) in at least two cycles of observation thus providing stereo views of the coronae. Stereo views are often critical in interpreting the geology in terms of establishing superposition and embayment relationships. To understand better the local and regional topographic context we also used Magellan altimetry, making contour maps and 3-D color images of the six coronae and their surroundings (Figure 2).

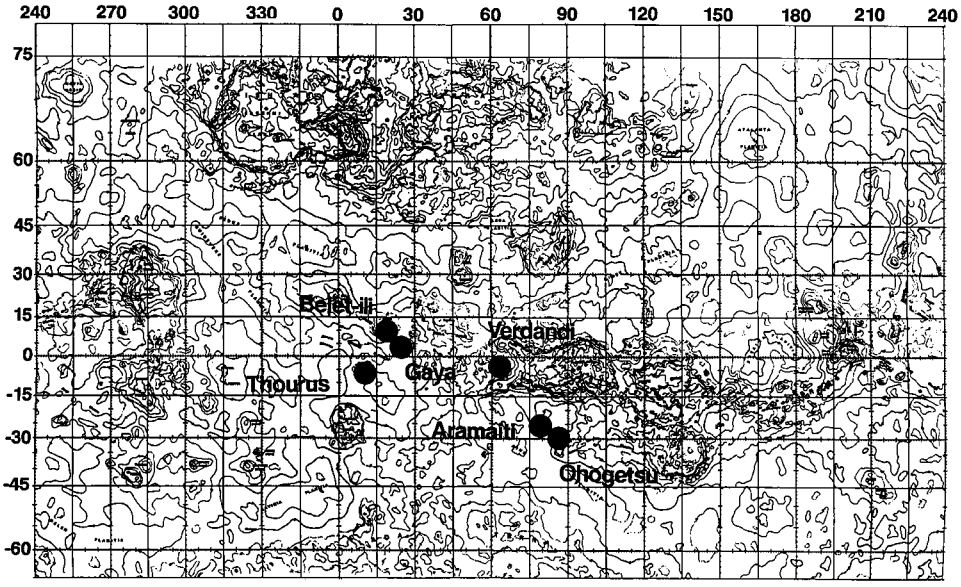

Figure 1. The locator map of six coronae studied in this work. The background is the topographic contour map.

2. Model of Regional and Global Stratigraphy of Venus

In this study we analyzed the age sequences of components of different coronae and correlated these with age sequences of regional and, if possible, global geologic units and the structures deforming them. Thus, we briefly review here the main characteristics of the model of regional and global stratigraphy of Venus as proposed initially by Basilevsky and Head (1994, 1995a–c). Following this initial analysis, a number of workers, including us, published new results of geologic mapping, and corresponding stratigraphic models for several areas of Venus (Aubele, 1995, 1996; Basilevsky, 1995, 1996a,b, 1997; Basilevsky and Head, 1996a,b; Basilevsky et al., 1997a,b; Copp and Guest, 1995; Gilmore et al., 1997; Head and Ivanov, 1996; Ivanov and Head, 1996; Jackson et al., 1996; Kryuchkov, 1996; Plaut, 1996; Saunders, 1996; Senske, 1996; Stofan and Guest, 1996). These new results are generally consistent with our stratigraphic framework and also led to some additions, clarifications, and modifications (Basilevsky et al., 1997a). This revised model subdivides the observed geologic formations of Venus into several groups and is useful as a framework for the stratigraphic assessment of the coronae analyzed (Figures 3 and 4). We describe it in ascending stratigraphic order:

(1) Fortuna Group: This includes the material of tesserae (Tt) which are large and small blocks standing above the surrounding plains whose surface morphology is characterized by at least two intersecting systems of ridges and grooves of evident tectonic origin. Tessera material is overlapped and embayed by all plains units described below.

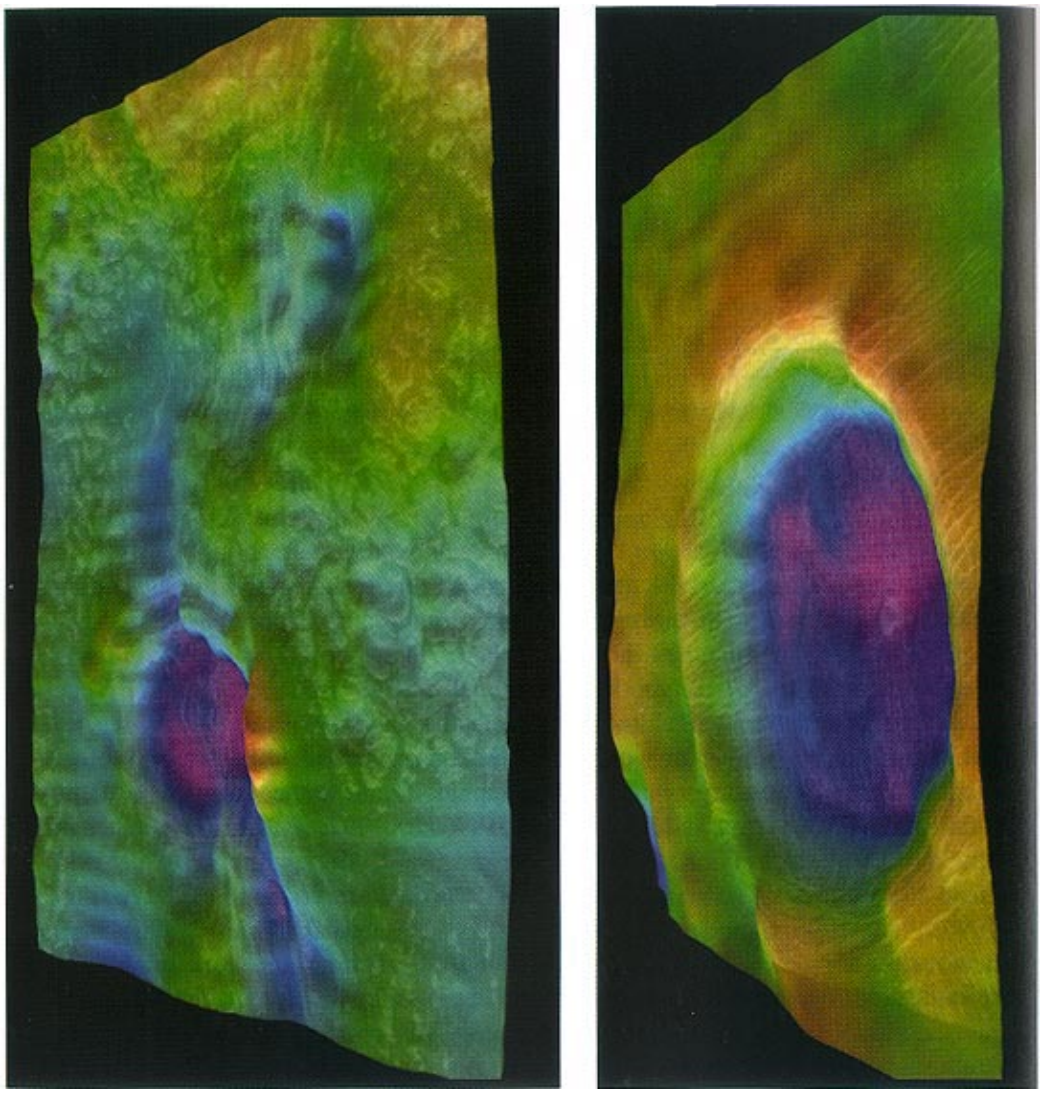

Figure 2a–b.

Figure 2. Three dimensional, color-coded oblique views of coronae treated in this study and their surroundings. We applied a smoothing procedure by taking the average of the eight pixels surrounding each pixel of the altimetry and replacing the center pixel with this average. Purples are lowest elevations, blues and greens, intermediate elevations, and yellows and reds, highest elevations. (a) Verdandi Corona, viewed from the south. (b) Thourus Corona, viewed from the south. (c) Belet-ili Corona and Gaya Corona, viewed from the south. (d) Ohogetsu Corona and Aramaiti Corona, viewed from the south.

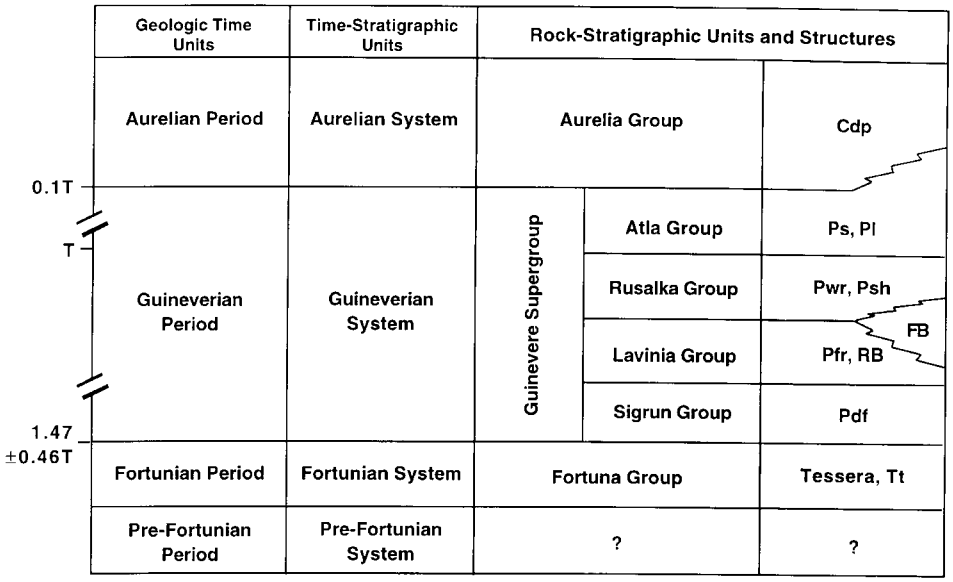

Figure 3. Stratigraphic column for geologic units and structures described in the text. Modified from Basilevsky and Head (1995a–c).

(2) Sigrun Group: This is represented by the material of densely fractured terrains of plains (Pdf) which embay tessera and is overlapped and embayed by the materials of younger plains.

(3) Lavinia Group: This is represented by the material of fractured and ridged (with rather broad ridges) plains (Pfr). Sometimes the ridges are clustered forming ridge belts (RB). Part of fractures which are often in this material are a result of its deformation, while some of the fractures observed in this unit are small remnants of Pdf material too small to be mapped at this scale. Lavinia Group material is overlapped and embayed by the materials of the younger plains.

(4) Rusalka Group: This is represented by the material of plains with wrinkle ridges (Pwr) which is typically so abundant on the surface of Venus that it forms a kind of the background terrain overlying and embaying older materials and is locally overlapped by patches of younger materials. Pwr plains typically have relatively low radar backscatter (they are moderately dark on the images) but mottled and even radar-bright varieties are also observed. These varieties often show distinct age relations among them so they may be considered as stratigraphic subunits of unit Pwr (e.g., Basilevsky and Head, 1996a; Head and Ivanov, 1996). However, global-wide correlation of these subunits is a task for future studies. The Pwr plains are covered with a network of wrinkle ridges that is a characteristic feature of them.

The Rusalka Group also includes material of plains formed by clustered and coalescing gently sloping volcanic shields (Psh). In most cases, this unit is em-

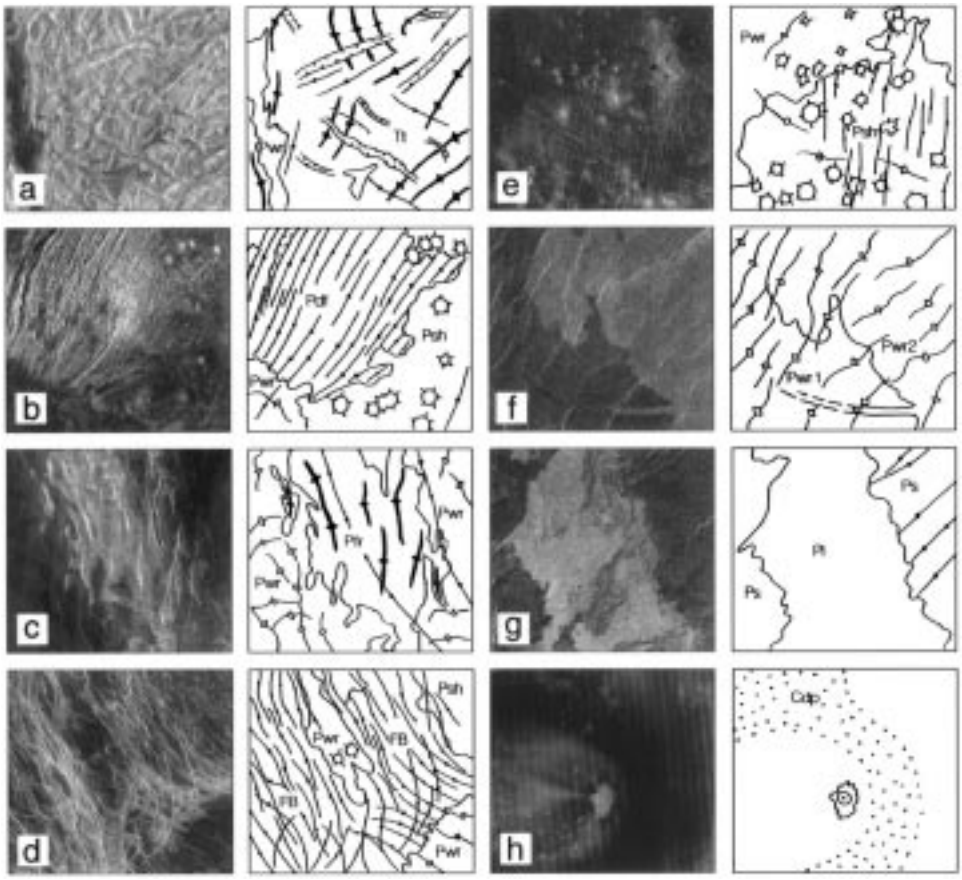

Figure 4. Typical examples of the proposed stratigraphic units. Thick lines with diamonds are ridge crests. Thin lines with diamonds are fractures. Wavy lines with open diamonds are wrinkle ridges. Paired thinner lines with inward facing hatchures are troughs interpreted to be graben. Circles with outward facing hatchures are small shields interpreted to be of volcanic origin. Thin solid lines are contacts, dashed where uncertain. (a) Tessera terrain embayed by plains with wrinkle ridges (Pwr) at 38.8°N, 75.8°. Portion of C1-MIDRP.45N074;1. Width of image is 165 km. (b) Densely fractured plains (Pdf) embayed by plains with shields (Psh), which in turn is embayed by plains with wrinkle ridges (Pwr), at 44.5°N, 335°. Portion of C1-MIDRP.45N329;1. Width of image is 60 km. (c) Fractured and ridged plains (Pfr) embayed by plains with wrinkle ridges (Pwr) at 41°N, 193.5°. Portion of C1-MIDRP.45N202;1. Width of image is 160 km. (d) Northwest-trending fracture belt (FB) embayed by plains with shields (Psh) and plains with wrinkle ridges (Pwr) at 38.5°N, 289.8°. Portion of C1-MIDRP.45N286;1. Width of image is 100 km. (e) Plains with shields (Psh) embayed by plains with wrinkle ridges (Pwr) from the northwest, at 44°N, 332.2°. Note the kipukas of shields flooded by Pwr near the contact with Psh. Portion of C1-MIDRP.45N329;1. Width of image is 100 km. (f) Plains with wrinkle ridges with low radar brightness (southwest, Pwr1) embayed and flooded by radar bright plains with wrinkle ridges (Pwr2), at 53°N, 177°. Note that channel formed in Pwr1 is embayed by Pwr2. Portion of F-MIDRP.55N180;1. Width of image is 70 km. (g) Smooth radar-dark plains (Ps) embayed by lobate radar-bright plains (P1) at 46°N, 243°. Portion of C1-MIDRP.45N244;1. Width of image is 100 km. (h) Impact crater (bottom center) with radar dark parabola (Cdp, indicated by stippled pattern) overlying all units, at 10°N, 76.2°. Portion of C1-MIDRP.15N077;201. Width of image is 450 km.

bayed by Pwr plains, but in a few cases the unit overlaps with early Pwr plains, and in some cases the relations with Pwr are ambiguous. This material was earlier described as a separate Pd stratigraphic unit in Navka Planitia by George McGill (in Solomon et al., 1992), as well as by Ivanov (1993) in the vicinity of Alpha Regio, Aubele (1995, 1996) within Vellamo Planitia, and by Basilevsky (1996a) in Beta Regio.

(5) Atla Group: This is represented by materials of smooth and lobate plains (Ps/Pl) which overlap and embay older materials and are not deformed by wrinkle ridges.

(6) Aurelia Group: This is represented by the material of radar-dark parabolas (Cdp) associated with the youngest impact craters (Campbell et al., 1992; Strom, 1993) as well as by the material contemporaneous with them but not necessarily associated with them, such as eolian patches (Sp) and streaks (Ss).

In mapping some areas of Venus we identified material of Fracture Belts (FB). These belts of dense fracturing are typically among the Pwr plains and most of the fractures are overlain and embayed by Pwr material while a few fractures appear to cut it. Within the Fracture Belts materials of the Sigrun, and Lavinia Groups, and parts of the Rusalka Group, may be present in a heavily deformed state.

And finally, in practically all large regions of Venus, impact craters lacking associated dark parabolas are present. Materials of their walls, floors, central peaks, rings and ejecta are usually designated as undivided crater material (Cu). In principle, these individual craters can belong to any group from Fortuna to Atla. However, because the majority of the observed impact craters are superposed on Pwr plains (including on the wrinkle ridges) and lack radar-dark parabolas, the materials of these craters should probably be considered as belonging to Atla Group.

The sequence of geologic units described above is, of course, a model. Many geological and stratigraphic analyses of Venus to date (Senske et al., 1994; Basilevsky and Head, 1995a–c; Tanaka et al., 1997) have observed this general sequence from tesserae to fractured and ridged plains and further to smooth and lobate plains. But what is the evidence for the broad synchroneity of these units (that is, that the same unit (e.g., Pwr) formed at approximately the same time in different areas of Venus)?

(1) The first line of evidence derives from the conclusion that if the stratigraphic sequences identified by us in different areas of Venus were not correlated in the temporal sense, and that the same units in the stratigraphic columns of different areas were not quasi-synchronous, then this would inevitably lead to the superposition of one unit sequence onto another unit sequence. For example, somewhere tessera of the younger sequence should overlap Pwr or Pl plains of the older sequence and so on. We did not observe this situation in any of the thirty-six 1000×1000 km areas of Venus studied (Basilevsky and Head, 1995a–c) and no observation of that sort is yet known to us from the publications of other authors.

(2) Second, photogeological analysis of the large region surrounding the 6800 km long lava channel Baltis Vallis (Basilevsky and Head, 1996a) provides additional information. This channel is considered to be formed geologically instan-

taneously (Kargel et al., 1994), thus making it an ideal stratigraphic marker. We considered the age relations among various stratigraphic units themselves in different parts of this region and then their age with respect to Baltis Vallis. On the basis of this analysis, it was possible to demonstrate the quasi-synchronous nature of the key stratigraphic units within this large region (∼1/20 of the entire surface of Venus) (Basilevsky and Head, 1996a).

(3) Third, photogeologic mapping of northern Venus (north of 35°N) (Basilevsky et al., 1997b) showed that the Pwr unit could be traced practically continuously throughout all the mapped area (about 115 of the surface of Venus). Then, using it as a stratigraphic marker to test the consistency of age relations among the associated stratigraphic units, it was found that the stratigraphic sequence was the same as reported earlier for this entire very large region. The same was found in the mapping of a strip of C1-MIDRs completely around the planet at 30 degrees north latitude (Ivanov and Head, 1997a,b). Keeping in mind that these two mapping projects covered the entire surface of Venus north of 22.3°N with continuous mapping, this, in combination with evidence from the first point, strengthens the conclusion of synchroneity even more at least for this ∼30% of the surface of Venus.

(4) The fourth point is closely related to third. An estimation of the time scale of emplacement of plains with wrinkle ridges was made based on consideration of the number of craters embayed by the Pwr plains, the crater rim heights, the implications for thickness of plains-forming material, and the bombardment rate (Collins et al., 1997). On the basis of this approach, Collins et al. (1997) estimated a relatively short (5–30 m.y.) time span for the emplacement of Pwr plains. This estimate per se constrains only the timespan of the Pwr emplacement but it does not exclude possible deviations from synchroneity among the same units of the stratigraphic columns of different areas of Venus.

These four lines of evidence support, but do not prove for the whole planet, the model of regional and global stratigraphy of Venus described above. Further analysis of this approach will come with the completion of synoptic (1 : 10M) geologic mapping of the planet in the future. On the basis of agreement with numerous studies in regions comprising a large percentage of the surface of the planet, we feel confident in using this terminology and stratigraphic scheme in this analysis.

In this paper we present the results of the detailed geological mapping of six coronae (Figure 1) chosen on the basis of their range of morphology and the availability of multiple cycles of Magellan image data to provide stereo coverage and variations in viewing geometry helpful in establishing stratigraphic relationships. These coronae cover most of the range of characteristics of those classified by Stofan et al. (1992) and are distributed in a range of geologic environments and settings (Figure 1). We first present the detailed descriptions, assess the stratigraphic position of the mapped units, and then discuss the implications for global stratigraphic units and coronae evolution.

3. Coronae Description and Regional Stratigraphic Relationships

In the descriptions given below, corona coordinates and size are according to Stofan et al. (1992), and confirmed by us. We prepared stereo images and digital images with altimetry and physical property overlays and used these to define geological units and determine structural and stratigraphic relationships. We compiled extensive geological descriptions of the nature and distribution of units and structures and their relationships. We now present a summary of the key characteristics.

1. *Verdandi Corona:* (Concentric, 5.5°N, 65.2°E, D = 180 km): Verdandi sits in a deposit of radar-dark plains with wrinkle ridges (Pwr) in the central part of Ovda Regio tessera massif (Figures 1, 5). The plains and tessera are darkened here by material probably associated with crater Andreianova (2.97°S, 68.76°E, D = 71 km). Tessera terrain in this area has a polygonal structural pattern which is very similar at least within an area of about 1000 × 1000 km around Verdandi corona. The closest distance between the corona annulus and tessera is east of the corona where the annulus and outcrops of tessera material are separated by 5 to 20 km of plains with wrinkle ridges (Figure 5b). No influence of the tessera structural pattern is seen in any elements of the corona including the area where the distance from the corona annulus to tessera is minimal. Plains with wrinkle ridges (Pwr) occupy almost all the area inside the corona annulus. It is well seen in stereo (Figure 6) and in the altimetry (Figure 2) that Pwr plains of the corona interior are generally lower in elevation than the Pwr plains exterior to the corona.

Three quarters of the corona annulus is made of densely fractured terrain (COdf) with an almost perfect concentric trend. Typical spacing of the concentric fractures is about 1 km. The annulus stands above the surrounding Pwr plains by 300 to 1000 m (Figure 2). In the southern and SE half of the annulus a prominent concentric ridge made of COdf is well shown in stereo in the form of the annulus rim crest. East of the corona, its annulus and outcrops of tessera material are separated by only 5 to 20 km of plains with wrinkle ridges. No influence of the tessera structural pattern is seen here in the annulus but in the blocks of tessera closest to the corona the concentric corona structural trend is partly developed.

Further to the SW, about 100–120 km from the corona, there is a field of small shields often with summit craters sitting mostly among the tessera; this field, lying outside the mapped area, is too small to be mapped at the scale of Figures 5 and 6 but appears similar to the shield plains (Psh) distinguished in some areas of Venus as a separate stratigraphic unit. The age relations of this shield field with Pwr plains are not very clear, but at least in one place (6.5°S, 64.1°E) a shield of about 5 km diameter is cut by fractures which do not continue Into the neighboring Pwr plains, so at least here the Psh seems to predate Pwr plains.

In the western sector there is a gap in the COdf annulus (Figures 5, 6). Here, Pwr plains neighboring the corona from outside to the west are continuous with Pwr plains of the corona Interior. At this place a set of younger fractures cut the Pwr plains to form a continuation of the corona annulus (Figure 5b). A set

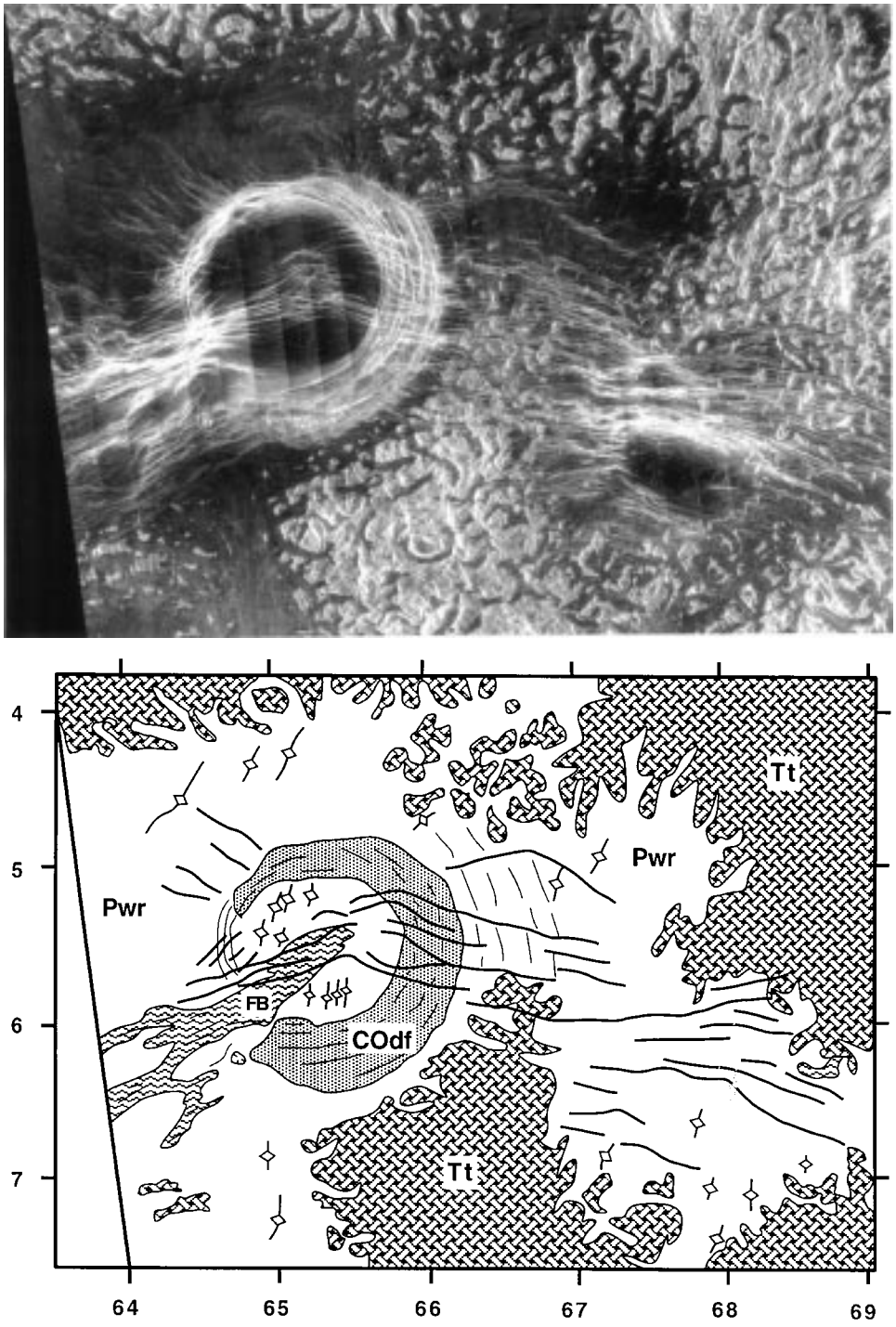

Figure 5. Verdandi Corona: (a) Magellan image, fragment of C1-MIDRP-00N060; 1. (b) Schematic geologic map. See text for unit designations; lines with diamonds are wrinkle ridges, thin and thick solid lines are fractures and faults of smaller and larger prominence. Area is 370 × 500 km.

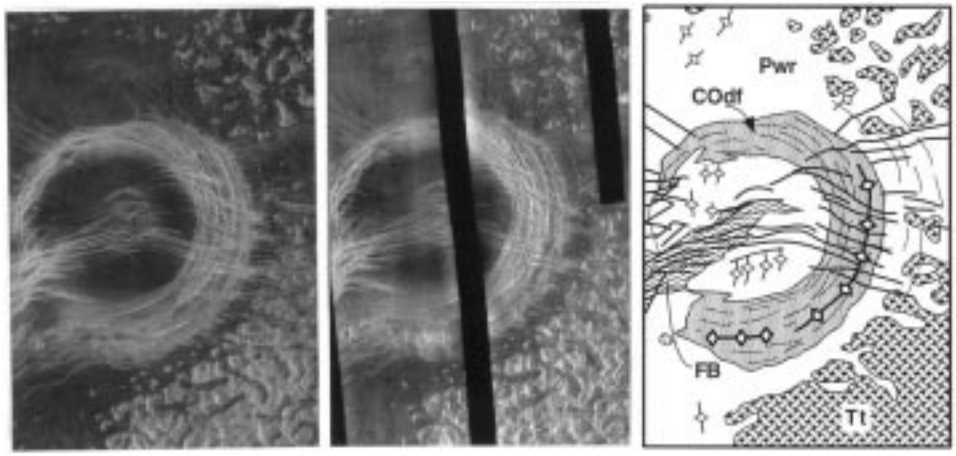

Figure 6. Stereopair of Verdandi Corona and its closest surroundings; fragments of F-MIDRP-05S065;1 and F-MIDRP-05S065;301, with schematic geologic map of the imaged area; see text for unit designations. Area is 210 × 280 km.

of relatively young fractures also criss-cross the Pwr plains of the corona interior and also the COdf corona annulus, and extend from the eastern part of the annulus to the surrounding Pwr plains and tessera. This set of fractures is associated with a topographic trough a few-hundred meters deep. Part of the fractures of this set appear embayed by Pwr plains while some of them appear to cut these plains. This situation is typical for fracture belts (FB), as mentioned above in the description of general stratigraphy. East of the corona a set of narrow fractures concentric to the corona cuts plains with wrinkle ridges (Pwr) including the wrinkle ridges themselves. The wrinkle ridges that complicate the surface of the Pwr plains both inside and outside the corona annulus trend mostly N-S and NE and show no alignment with the structural pattern of the corona.

In summary, the sequence of events deduced from these units and structures and their relationships in the area under study (Figures 5, 6) are as follows:

(1) Emplacement of tessera material and its deformation into what we see now as tessera terrain.

(2) Emplacement of the material seen now as the densely fractured terrain of Verdandi corona annulus (COdf) and its intense concentric deformation. This unit is probably correlative with the Pdf geologic unit of Basilevsky and Head (1995a–c), and it underwent subsequent concentric fracturing supposedly simultaneously with the dense fracturing typical of the Pdf unit. This is the first identified stage of corona formation. On the basis of the geologic record preserved in this area, it is not clear what was happening here when in many other areas of Venus emplacement of the Pfr plains and their warping into ridge belts (RB) was taking place.

(3) Emplacement of the material of plains with wrinkle ridges (Pwr) and its deformation by the wrinkle ridges. The N-S to NE trends of the wrinkle ridges appear

not to be in alignment with the corona structure; this may mean that the active evolution of Verdandi was largely over by this time. Formation of the topographic rise of the corona annulus certainly predated the emplacement of Pwr plains because our observations show that the plains material embayed the topographic rise of the annulus which already existed. The floor of this corona, covered with material of the Pwr plains visible now, seemed to be at least partly downwarped below the level of the surrounding plains when the wrinkle ridges deforming them were already emplaced.

(4) Formation of the set of narrow concentric fractures seen east of the corona. Strictly speaking this set is an element of this corona, so the corona evolution was continuing even after the emplacement of wrinkle ridges, but it was probably a passive readjustment of the corona surroundings to the presense of corona topography, or the response of the corona exterior to the late subsidence of Pwr in the corona interior.

(5) Formation of the set of regional fractures cutting both the corona annulus and the wrinkle ridged plains of the corona interiors and surroundings.

The set of the FB-type fractures probably partly predated and partly postdated the emplacement of the Pwr plains. The topographic trough associated with this fracture belt was evidently formed after the emplacement of Pwr plains; otherwise it would probably be filled with their flow material.

2. *Thourus Corona:* (6.5°S, 12.9°E, D = 290 km; Figures 7–9): Thourus corona is located north-northeast of Alpha Regio in southern Tinatin Planitia (Figure 1). The Thourus corona annulus is mostly made of densely fractured terrain (COdf) and has an almost perfect concentric pattern (Figures 7–9). The spacing of the concentric fractures is about 1 km and less. The COdf corona annulus completely encircles the corona. It is well seen in stereo (Figures 8, 9) and in the altimetry data (Figure 2) that the eastern part of the annulus noticeably stands above the surrounding plains (by ∼300 m) while in the western part of the annulus there are two places where the topographic expression of the annulus is less prominent (less than 100 m). The corona interior is lower than the surrounding plains by about 400–600 m.

The densely fractured ring of the corona anulus is embayed by materials of three types. First, and stratigraphically oldest, is material which is a part of the topographically prominent section of the corona annulus in its northern and southern sectors. It has a relatively smooth surface morphology bearing no prominent concentric fracturing typical for COdf and is embayed by the material of plains with wrinkle ridges. This material is crossed by a set of relatively short NW-trending fractures which also cross the adjacent COdf material and the material of shield fields nearby, but Pwr plains bury the fractures. Although age relations of this material with the shield plains are unclear because they are not in a direct contact, the fact that this material embays the COdf component and is embayed by the Pwr plains is an indication that it might be correlative with the fractured and

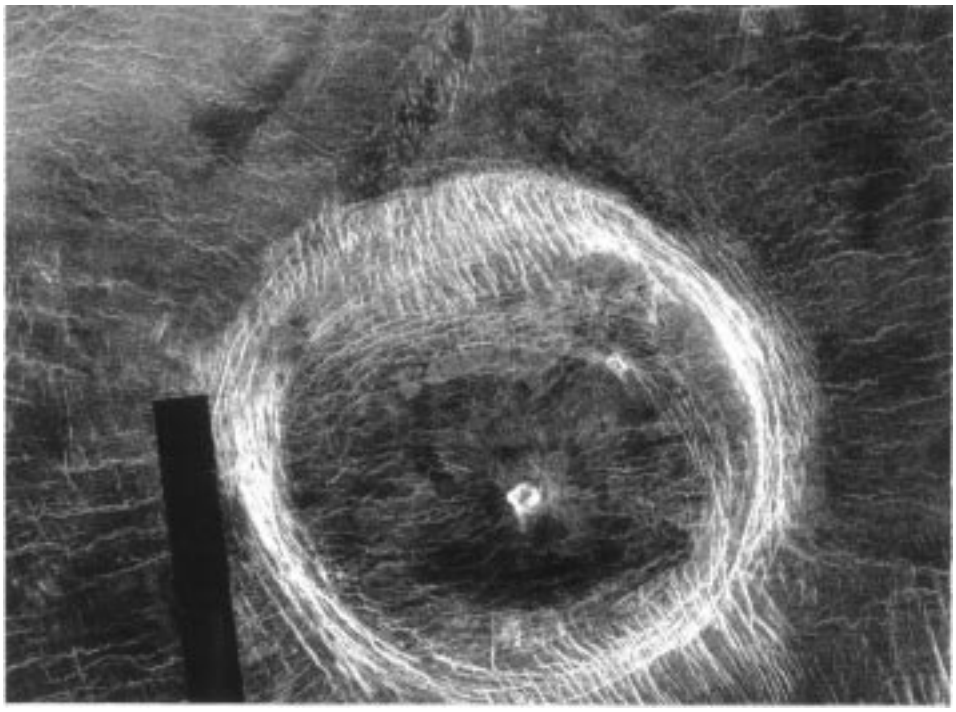

Figure 7. Thourus Corona:: (a) Magellan image, fragment of C1-MIDRP-00N009;1. (b) Schematic geologic map. See text for unit designations; lines with diamonds are wrinkle ridges, thin solid lines are fractures. Area is 220 × 300 km.

ridged plains unit (Pfr) while the fractures crossing it may be contemporaneous with the pre-Pwr fractures of the fracture belts (FB).

The next unit is material of two fields of small volcanic shields. One is in the eastern sector of the corona interior and the other is in the center of the corona interior. The second field contains a relatively large (about 15 km across) prominent dome with summit crater a few km in diameter. This material is crossed by the set of NW-trending fractures which do not extend into the surrounding plains with wrinkle ridges. These two occurrences thus predate Pwr and are probably a correlative of shield plains (Psh). This material is also present in the vicinity of the area under study without association with this or other coronae.

The last of three units is material of plains with wrinkle ridges (Pwr) which form both the corona surroundings and the dominant part of the corona interior, embaying the COdf component of the corona annulus. The plains have radar-dark patches with diffuse boundaries probably due to the local mantling by material ejected from the impact crater Carreno (3.90°S, 16.10°E, D = 58.5 km). Pwr plains are deformed by wrinkle ridges with a predominantly E-W trend. East and west of the corona the orientation of the ridges is slightly deflected from the E-W direction

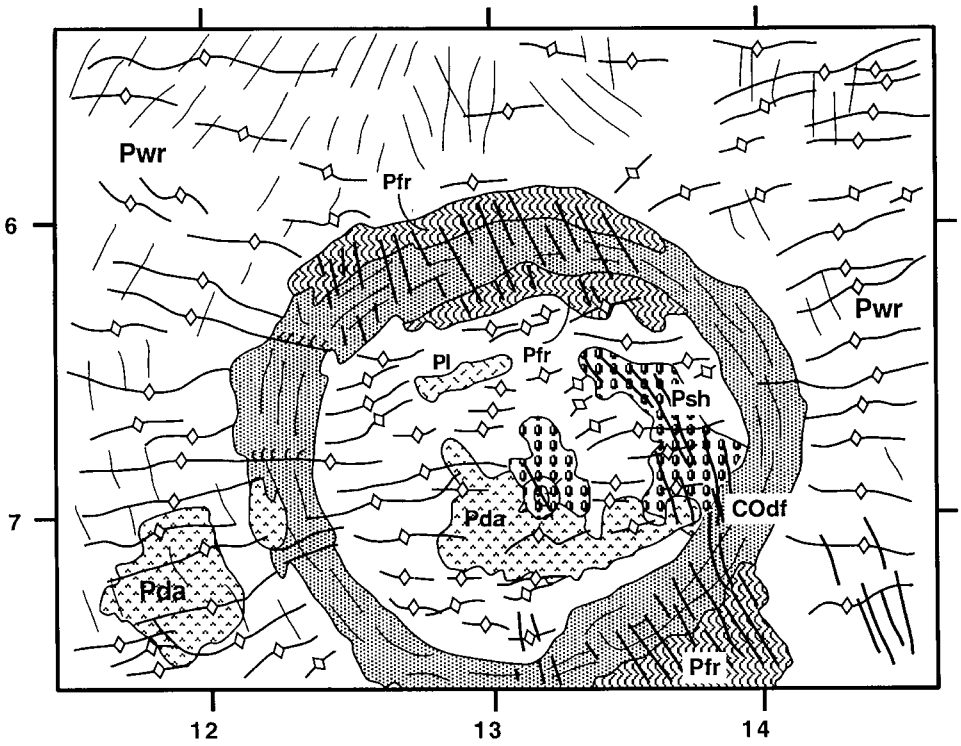

Figure 7. Continued.

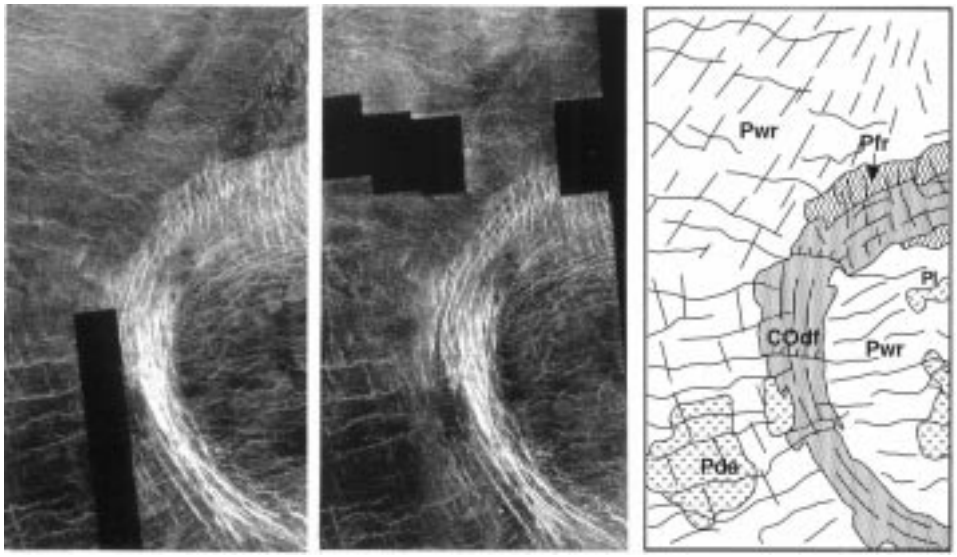

Figure 8. Stereopair of the western part of the Thourus Corona; fragments of C1-MIDRP-00N009;1 and C1-MIDRP-00N009;301, with schematic geologic map of the imaged area; see text for unit designations. Area is 130 × 240 km.

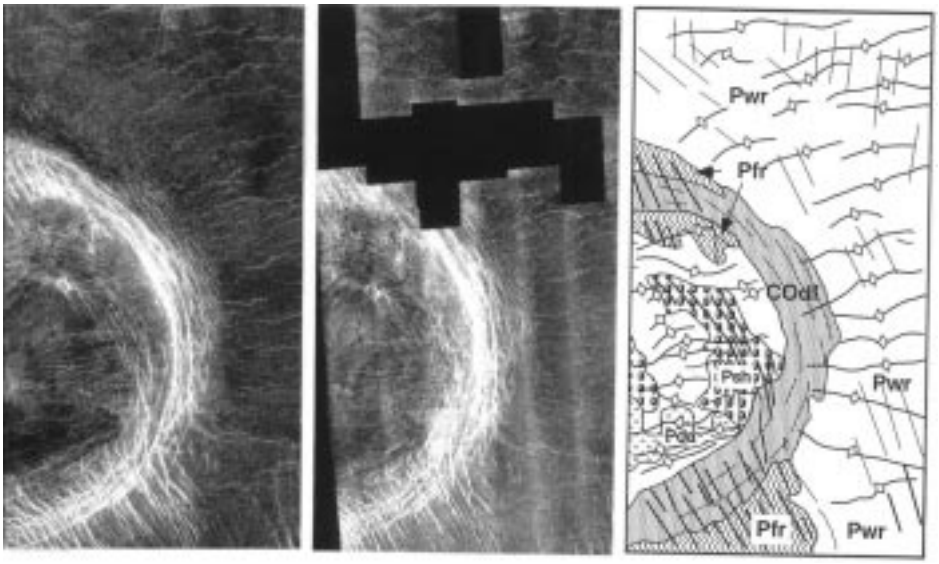

Figure 9. Stereopair of the eastern part of Thourus Corona; fragments of C1-MIDRP-00N009;1 and C1-MIDRP-00N009;301, with schematic geologic map of the imaged area; see text for unit designations. Area is 130 × 240 km.

towards a direction radial to the corona. Wrinkle ridges inside the corona also show a very slight deflection to directions radial to the corona center.

Wrinkle ridges in the mapped area are very serpentine at small scale, probably due to the presence of fine, densely-spaced NW to NE trending lineaments (fractures?) crossing the plains. The fractures probably predated and controlled the emplacement of wrinkle ridges. Wrinkle ridges cross not only the Pwr plains, but also COdf and Psh. It is well seen in stereo that wrinkle ridges crossing the western part of the corona annulus merge into prominent scarps.

Within Thourus about 50 km NW of the corona center there is an E-W elongated (10 × 50 km) area of relatively bright plains not deformed by, and thus younger than, the wrinkle ridges. This material appears to be flow(s) of lava and is probably correlative with the lobate plains (Pl) unit of Basilevsky and Head (1995a–c). In the southern part of the interior, smooth dark plains may represent some of the latest volcanic activity, and be correlative with amoeboid plains (Pda).

In summary, the sequence of events determined from the units mapped in the Thourus corona area is as follows:

(1) Emplacement of the material now forming the COdf component of the corona annulus and its deformation by a dense set of concentric fractures. This is the visible beginning of formation of the corona. Based on the age relations with other units of the area described above, this material is evidently correlative with the densely fractured plains (Pdf) unit.

(2) Emplacement of the material which is considered to be correlative with the Pfr regional unit and its involvement in the formation of the topographic prominence representing the corona annulus.

(3) Emplacement of the material of fields of small shields and the larger dome with summit crater, all of which appear to be correlative with the Psh regional unit.

(4) Local NW-trending fracturing of COdf, Pfr and Psh materials.

(5) Volcanic eruptions which formed the regional Pwr plains and similar plains in the corona interior. This material was first finely fractured and then warped by compressional deformation into a set of wrinkle ridges which, when approaching the corona, changed their orientation to radial. The latter is evidently a result of superposition of the regional ridge-forming stress and local corona-associated stress which appeared to be due either to active local tectonism or to passive influence of the previously existing corona topography. Subsidence of the corona interior may have continued into this period.

(6) Subsidence of the corona interior.

(7) Finally, there was an episode of volcanism which emplaced the lobate plains in the northern part of the corona interior and the amoeboid plains in the southern part of the corona interior. This was the last visible signature of the evolution of Thourus corona, although some subsidence may have continued past this time.

3. *Belet-ili Corona:* (Concentric; 6.0°N, 20.0°E, D = 300 km; Figure 10): This corona, and adjacent Gaya corona to the SE, are situated about 2000 km east of Gula Mons among the plains (mostly Pwr) of southern Bereghinya Planitia (Figure 1). Belet-ili corona has an annulus consisting of different materials and structural features which together form the very visible circular structure seen in the images (Figure 10). In the altimetry data (Figure 2) the most prominent feature is not the annulus but the circular trough surrounding the central elevated part of the corona. The trough depth is about 300 to 500 m in relation to the plains outside the corona. The corona annulus rises above the surrounding plains from less than 100 m to about 300 m. The central elevated part of the corona interior stands 500 to 1000 m over the circular trough floor and 300–600 m over the plains outside the corona.

The western portion of the corona annulus (about 60° of arc; Figures 10, 11) is encircled by a topographically elevated rim composed of a plains-like terrain crossed by rare long fractures concentric to the corona structure as well as several small (a few km across) areas of densely spaced fractures appearing as inclusions of densely fractured terrain of coronae (COdf) described above (see descriptions of coronae Verdandi and Thourus). This plains-like terrain is most similar to fractured and ridged plains (Pfr) and is embayed by plains with wrinkle ridges (Pwr) which are dominant both in the corona surroundings and its interior. The topographic prominence and the embayment by Pwr plains are especially well seen in stereo. In the southern part of the arc of this terrain the latter embays a relatively small massif of tessera terrain.

About 20–30 km east of this 60° segment of the annulus there is another (smaller) arc of similar looking terrain, also embayed by Pwr plains and concentric to the

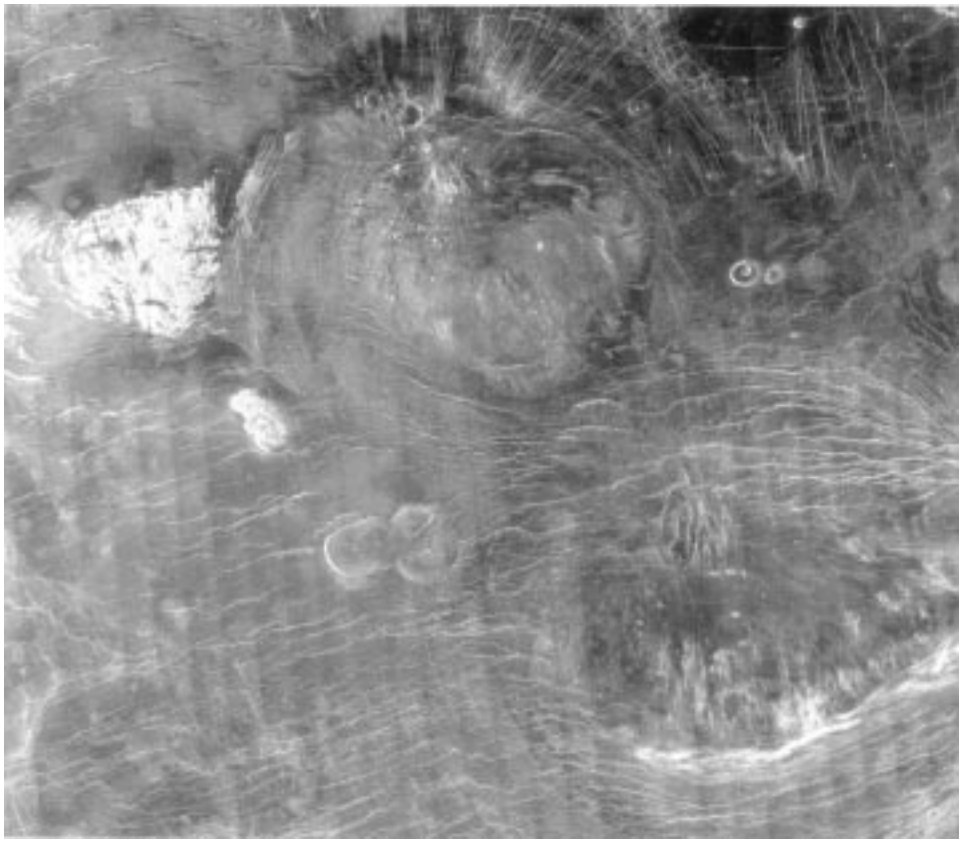

Figure 10. Belet-ili Corona (upper left) and Gaya Corona (lower right): (a) Magellan image F-MIDRP-05N026;2. (b) Schematic geologic map. See text for unit designations; lines with diamonds are wrinkle ridges, thin solid lines are fractures. Area is 500 × 570 km.

corona structure. In contrast to the first arc, this one has practically no topographic expression. The plains-like morphology, embayment by plains with wrinkle ridges, and presence of inclusions appearing as small areas of COdf, provides the basis on which to correlate the terrain within these two arcs with fractured and ridged plains (Pfr) of Basilevsky and Head (1995a–c).

The northern part of the corona annulus contains two systems of narrow intersecting concentric fractures and radial fractures, both cutting the coalescing shields forming shield plains and plains with wrinkle ridges, including the wrinkle ridges themselves (Figure 10). Some of the shields appear to be criss-crossed by wrinkle ridges while other shields appear to be overlapping them. Here, and more toward the interior of the corona, there are a few small pieces of densely fractured terrain of coronae (COdf) concentric to the corona and embayed by the Pwr plains.

In its eastern part Belet-ili corona has almost no annulus, although evidence of the trough can be seen in altimetry, and plains with wrinkle ridges (Pwr) dominate.

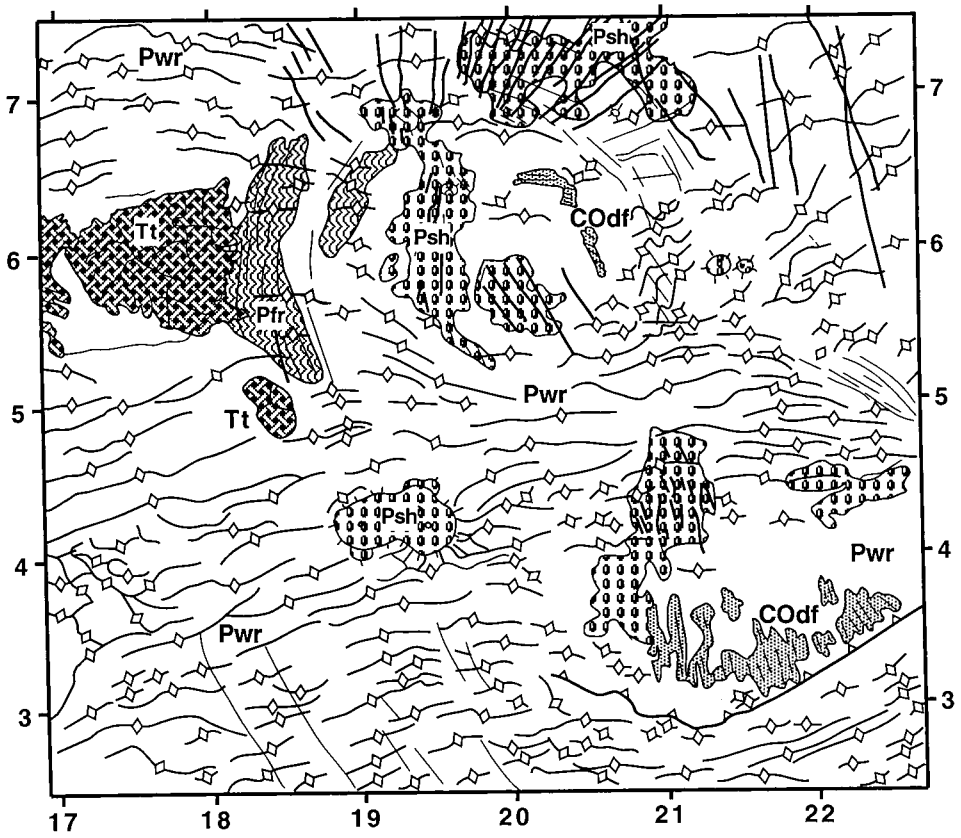

Figure 10. Continued.

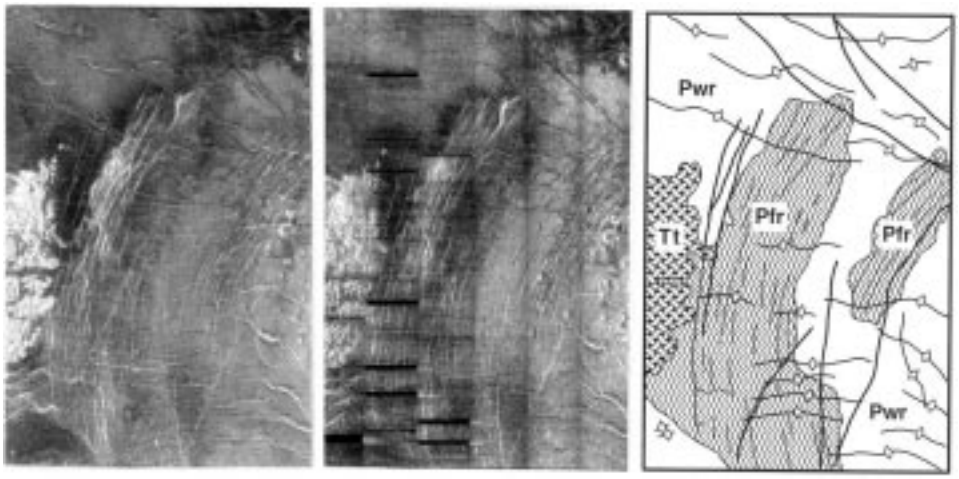

Figure 11. Stereopair of the northwestern part of the Belet-ili Corona annulus; fragments of F-MIDRP-05N026;2 and F-MIDRP-05N026;301, with schematic geologic map of the imaged area; see text for unit designations. Area is 130 × 180 km.

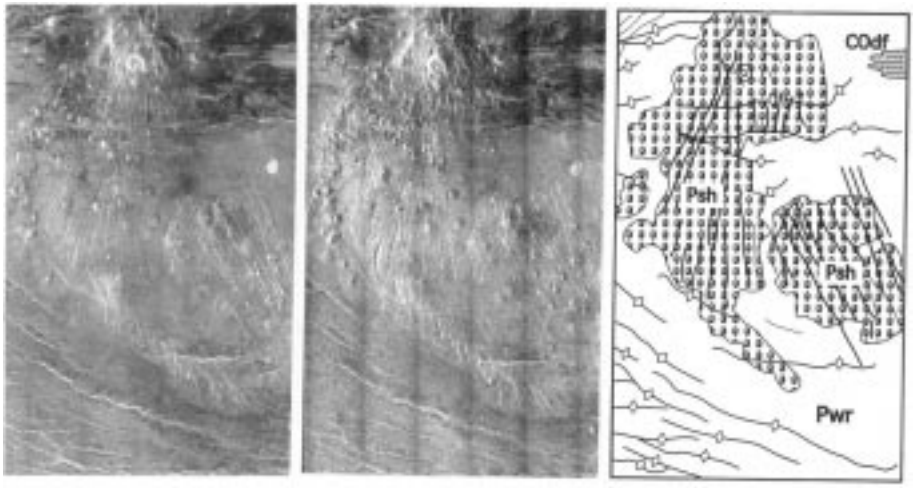

Figure 12. Stereopair of the central part of Belet-ili Corona; fragments of F-MIDRP-05N026;2 and F-MIDRP-05N026;2, with schematic geologic map of the imaged area; see text for unit designations. Area is 130 × 180 km.

The only evidence of the annulus is that E-W trending wrinkle ridges start to zigzag as they approach the place where the annulus should be. The southern part of the corona is outlined by wrinkle ridges. Their spatial density here is practically the same as in the corona vicinity but they are aligned in a somewhat concentric manner (Figure 10).

The central elevated part of Belet-ili corona (Figures 2, 12) is dominated by fields of numerous, often coalescing shields with an appearance very similar to the shield plains (Psh). The shields are typically of 1–5 km In diameter. About 70 km NW of the corona center there is a shield (about 12 km across) with a relatively large (5 km) caldera open downslope to the south. This shield sits at the southern slope of a prominent topographic rise about 40 km across and is also composed of Psh. The shield fields are crossed by sets of fractures radiating from the 40 km-topographic rise and this rise has the highest (among Psh) density of fractures. These fractures typically do not extend from the Psh areas into the surrounding plains with wrinkle ridges making the embayment of Psh by Pwr plains very evident. These fractures can be correlated in time with the upper, but not uppermost, component of fractures composing fracture belts (FB). One of the shield fields extends into the area of the northern segment of the annulus. In addition to typical shields it contains a circular caldera-like feature with a flat plains-like floor.

In summary, the sequence of events inferred from the units mapped in the area of Belet-ili corona is as follows:

(1) The initial event for which evidence is seen in this area was the emplacement of tessera material and its deformation into what we see now as tessera terrain.

(2) Emplacement of the material composing densely fractured terrain of coronae (COdf) (now seen as small inclusions in the NW and N sectors) and its dense

concentric fracturing. This is the first visible, but now poorly preserved, sign of the presence of Belet-ili corona activity.

(3) Emplacement of the correlative of Pfr plains and its involvement in the formation of the topographically prominent annulus of the corona.

(4) Emplacement of fields of small shields (Psh) and their fracturing into a system radial to the 40 km topographic rise. This system can also be considered as roughly radial to the corona structure although its focal point is offset from the geometric center of the corona.

(5) Emplacement of the plains with wrinkle ridges which flooded almost 300° of the corona annulus composed of Pdf and Pfr (assuming it was originally complete) and later were wrinkle ridged and then concentrically fractured. Both wrinkle ridges and concentric fractures together encircling almost all of the corona perimeter are the last visible signatures of activity of Belet-ili.

4. *Gaya Corona:* (Multiple, 3.5°N, 21.5°E, D = 400 km mean value): Gaya corona (Figure 1) is a pear-shaped structure in planimetric view, about 350 × 500 km in size. It is elongated in an E-W direction and outlined by sets of wrinkle ridges forming the 100–120 km wide corona annulus. In the eastern apical part of the corona (outside the area of Figure 10) there is a circular feature, mostly also formed by wrinkle ridges, fitting in the general outlines of the corona. The presence of this feature was evidently the basis on which Stofan et al. (1992) classified Gaya as a multiple corona. The material forming the annulus of Gaya corona is the same as the material of its surrounding: plains with wrinkle ridges (Pwr), although units with two different brightnesses are distinguishable. The darker one contains numerous patches of superposed low-backscatter material. The outer portion of the NW part of the Gaya annulus is simultaneously the southern part of Belet-ili corona annulus.

In the altimetry data (Figure 2), the most prominent segments of the corona annulus are the NE and SE parts, which are outlined from outside by the arcuate troughs concentric to the annulus. These segments of the annulus stand 600–1000 m over the trough floor and 300–600 m over the surrounding plains. The NW and SW segments of the annulus are much less prominent in the altimetry image data. The central part of the corona is elevated 300–600 m over the plains outside the corona. This elevated central part is separated from the annulus to the east, south and west by the trough, whose floor, in its deepest parts, is about 1500 m below the summits of the corona annulus rise.

The SW part of the annulus is also encircled by a set of concentric fractures of variable spatial density (Figure 10). They cut Pwr materials and may be the cause of large amount of small-scale sinuosity of wrinkle ridges in this region; if so, they evidently predate the wrinkle ridges.

The central part of Gaya corona also contains plains with wrinkle ridges (Figures 10, 13). Wrinkle ridges here are less spatially dense and less prominent than in the annulus. In addition, the corona interior contains densely fractured terrain (COdf) and fields of small shields (Psh) (Figure 13). It is readily observed in stereo

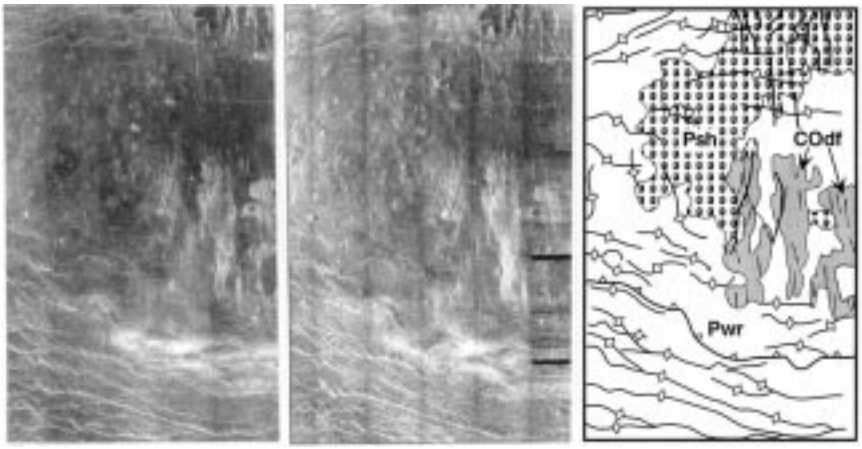

Figure 13. Stereopair of the southern part of Gaya Corona; fragments of F-MIDRP-05N026;2 and F-MIDRP-05N026;2, with schematic geologic map of the imaged area; see text for unit designations. Area is 130 × 180 km.

that the southern part of the corona interior is separated from the adjacent part of the annulus by a rather steep north-facing slope, which is almost a scarp. It is in perfect alignment with the local pattern of wrinkle ridges and this implies that both the slope and wrinkle ridges were formed in the same tectonic event.

Densely fractured terrain (COdf) form several patches in the same area and are embayed both by Pwr and Psh. The dense fracturing of COdf trends NNW and NW, thus appearing to be approximately radial to the general structure of this corona in this area.

Fields of small shields (Psh) in the corona interior are generally similar to those observed inside Belet-ili corona. They form two patches separated areally by plains with wrinkle ridges. The northern part of the western field is deformed by fractures. The Psh fields appear to be embayed by Pwr plains (Figure 13).

At the outer part of western segment of the Gaya corona annulus there are four coalescing steep-sided domes (Figure 14). At first glance they look superposed on plains with wrinkle ridges. Thorough analysis of stereo images showed, however, that the domes have fine wrinkle ridges in them and wrinkle ridges of the surrounding plains are arranged around one of the domes (the SE one) in a radial manner. But the most conclusive evidence for the stratigraphic position of the domes comes from the analysis of the NW slopes of the two westernmost domes. The slopes here have a scalloped morphology which Is interpreted to be the result of collapse and slumping of the slope materials, with obscuring the slump deposits by subsequent embayment by new formed plains (see Figures 5, 14a–d in Pavri et al., 1992; Bulmer, 1996). In the case of the dome cluster at the western margin of the Gaya corona annulus there is a typically scalloped slope and no slump deposits at the foot of the slope. A few km NW of the scalloped slopes there is a cluster of the NE trending wrinkle ridges. One interpretation is that these features are not wrinkle ridges but

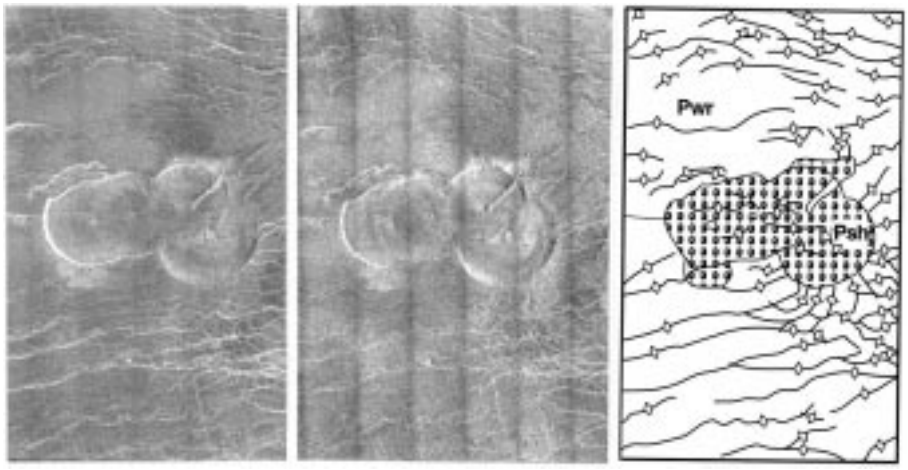

Figure 14. Stereopair of the dome cluster in the area of the western part of the Gaya Corona annulus; fragments of F-MIDRP-05N026;2 and F-MIDRP-05N026;2, with schematic geologic map of the imaged area; see text for unit designations. Area is 130 × 180 km.

peculiar-looking distal parts of slumped material; however, the space between this ridge cluster and the scalloped slopes is definitely embayed by Pwr material. On this basis we reach the conclusion that the dome cluster predated the emplacement of plains with wrinkle ridges. The dome cluster may be contemporaneous with the fields of small shields of this area.

In summary, the sequence of events in the area of Gaya corona is as follows:

(1) Emplacement of material of densely fractured terrain (COdf) and its roughly radial fracturing. This material is evidently correlative with the Pdf unit and its fracturing is interpreted to have been contemporaneous with the dense fracturing typical of the Pdf unit. It is not clear what was happening in this area when in many other areas of Venus, including the neighboring corona Belet-ili, there was an emplacement of the Pfr plains and their warping into ridge belts (RB).

(2) Emplacement of fields of small shields (Psh) (and their subsequent local fracturing) now seen inside the corona and emplacement of a cluster of the steep-sided domes domes at the corona western margin.

(3) Emplacement of regional plains with wrinkle ridges (which flooded most of the pre-existing elements of Gaya corona), their subsequent fracturing concentric to Gaya, and wrinkle ridging, as well as formation of the north-looking scarp separating the southern part of the corona annulus from its interior. Good agreement of the wrinkle ridge and the concentric fracture orientation with the corona topography is probably evidence that all of them were formed at about the same time period. This fracturing, ridging and formation of the scarp are the latest visible signatures of activity at Gaya corona.

5. *Aramaiti Corona:* (Concentric/caldera, 26.3°S, 82.0°E, D = 350 km): Aramaiti Corona is located south of Ovda Regio among the plains of Aino Planitia

(Figure 1). In the vicinity of the corona there are two major varieties of regional plains (Figure 15). They both are varieties of plains with wrinkle ridges (Pwr) described by Basilevsky and Head (1995a–c) as the most widespread regional stratrigraphic unit of Venus. One of the varieties has intermediate radar brightness (Pwr-i), another is noticeably darker (Pwr-d). Their relations with Aramati corona (see below) show that Pwr-i material is older than that of Pwr-d. Varieties of Pwr have been described elsewhere on Venus in Baltis (Basilevsky and Head, 1996a) and in the Venera 8 landing site area (Basilevsky, 1997). The network of wrinkle ridges is superposed on both subunits and boundaries between these two plains varieties definitely did not control the emplacement of these ridges.

Immediately east of Aramaiti Corona there is a belt of fractured and ridged plains embayed by both varieties of plains with wrinkle ridges (Pwr). It can be correlated with fractured and ridged plains (Pfr) described by Basilevsky and Head (1995a,b,c) in many regions of Venus. In its northern part this belt is embayed by a field of small shields. The latter looks very similar to shield plains (Psh).

Aramaiti Corona has a peculiar interior spiral-like form in planimetric view with its outer outlines forming an almost perfect circle (Figure 15). In its northern part Aramaiti has two annulae divided by an arcuate trough and only one annulus in the southern part. The central part of the corona, its core, is represented by prominent dome separated from the annulus by the concentric trough. The inner annulus of the northern part and the annulus of the southern part, which actually form together a single spiral, both are formed of densely fractured terrain (COdf) generally similar to terrains of this type of other coronae.

Aramaiti corona has a prominent topographic expression, well seen both in stereo and in the altimetry data (Figures 1, 16, 17). Its annulus stands 100–400 m above the surrounding plains. The southern segment of the annulus is higher than the northern one and outside of it there is a shallow trough, 100–200 m below the surrounding plains. In the northern part of the corona, the inner annulus stands 400–600 m over the nearby plains outside the corona while the floor of the trough between the outer and inner annulae is about 100 m below the plains. The corona core summit reaches the hypsometric level of the plains surrounding the corona, while the floor of the trough between the annulus and the core is 400–800 m below the plains.

A distinctive characteristic of this corona is that the COdf unit here can be subdivided into two subunits. Subunit COdf-a occupies the rim crest of the first third of the COdf spiral while subunit COdf-b occupies the rest. Both of them have perfect concentric fracturing. However, subunit COdf-a has a rougher surface. It consists only of alternating concentric ridges and troughs while subunit COdf-b has a visible smooth plain-like background saturated with fine concentric lineaments. Another difference which has an apparent stratigraphic significance is that COdf-a is embayed by Pwr-i, the lower subunit of plains with wrinkle ridges that is seen at the eastern and western terminations of the COdf-a band. COdf-b, on the other hand, gradually merges into Pwr-i; this is best illustrated at the western termination

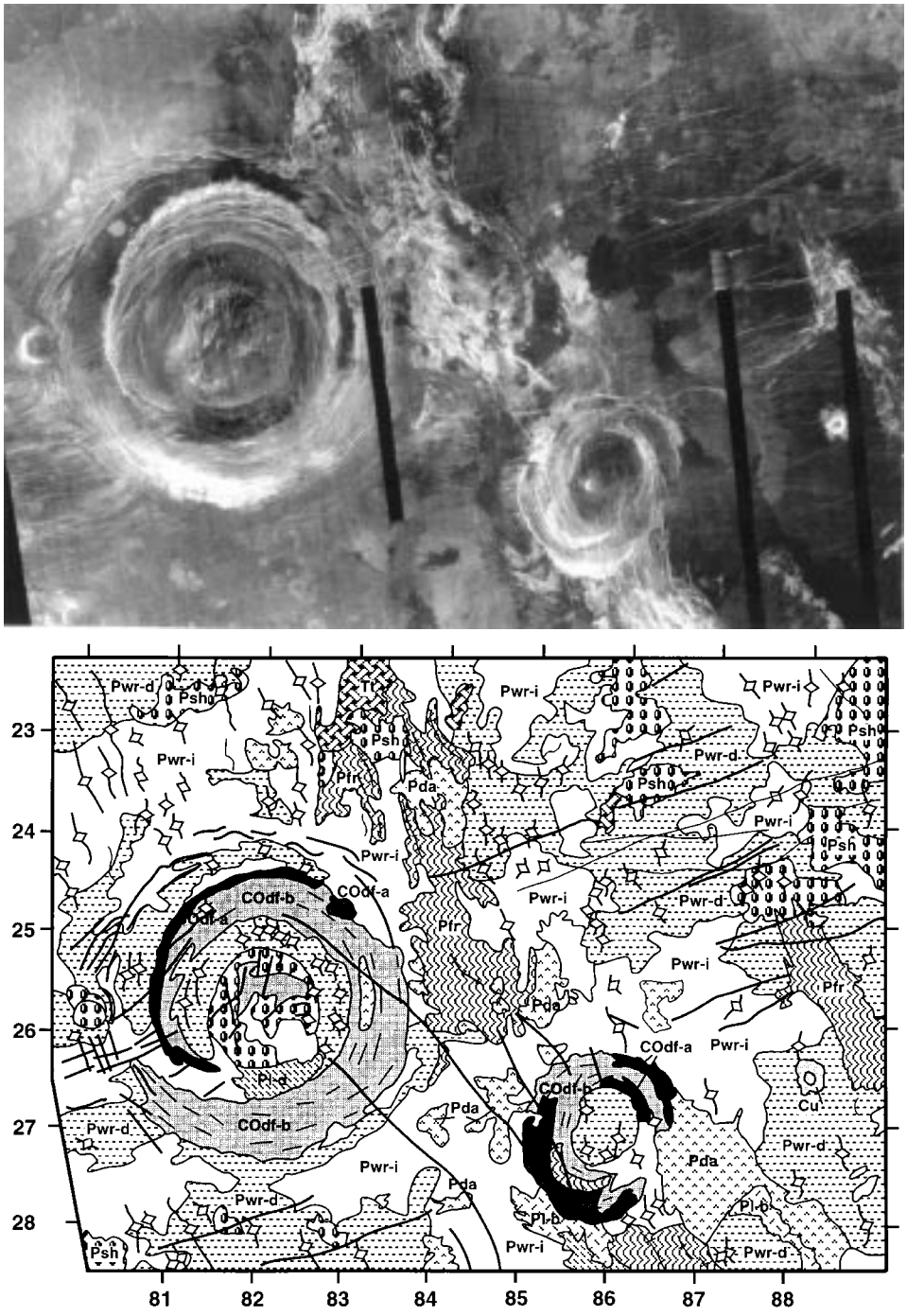

Figure 15. Aramaiti Corona (left) and Ohogetsu Corona (right): (a) Magellan image, fragment of C1-MIDRP-30S081;1. (b) Schematic geologic map. See text for unit designations; lines with diamonds are wrinkle ridges, thin and thick solid lines are fractures and faults of small and larger prominence. Area is 600 × 800 km.

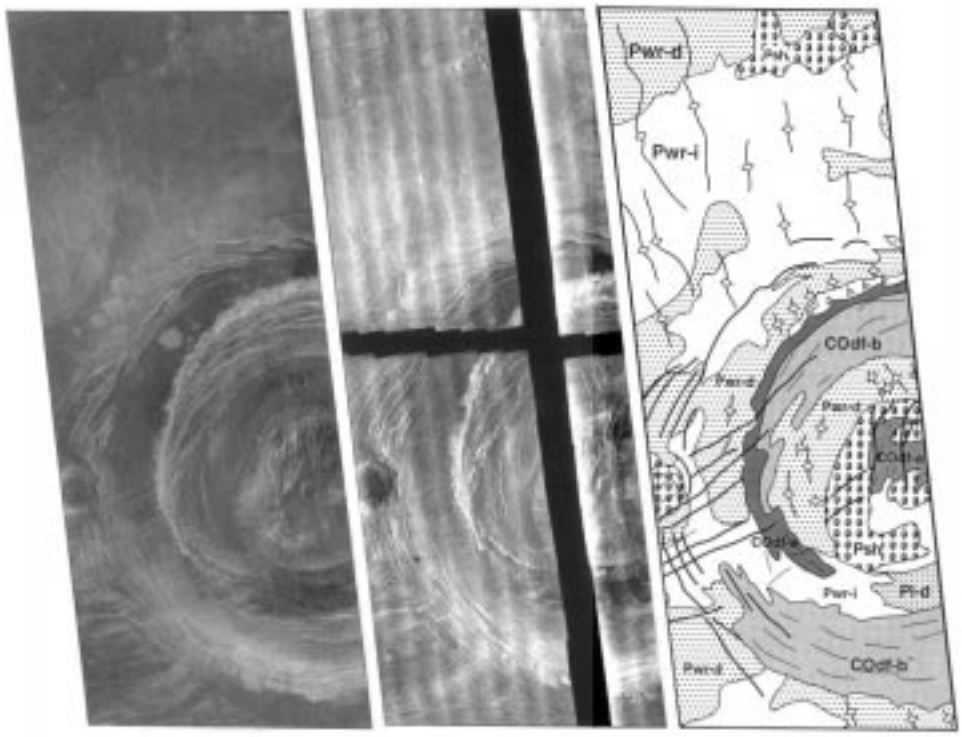

Figure 16. Stereo pair of the western part of Aramaiti Corona; fragments of F-MIDRP-25S082;1 and F-MIDRP-25S082;301, with schematic geologic map of the imaged area; see text for unit designations. Area is 200 × 500 km.

of the spiral and at the place where the outer part of the eastern segment of the annulus meets the neighboring Pwr-l plains. So COdf-b is apparently the result of deformation of regional Pwr-i material while COdf-a is made of older material and its deformation predated emplacement of the Pwr-i plains.

At the western part of corona the Pwr-i plains of the inter-annulus trough merge into the same plains of the corona surrounding. The outer annulus of the northern part of corona Aramaiti is made of Pwr-i plains (Figure 13). They are cut here by an approximately concentric set of partly sinuous faults. This faulted arc of plains gradually changes outwards into normal plains over a distance of about 30–40 km. The trough between the outer and inner annulae is filled with a relatively dark unit of plains with wrinkle ridges (Pwr-d) which embay both the faulted material of Pwr-i and the heavily deformed material of COdf-a. At the northern foot of the inner annulus, composed of COdf-a material, there is a narrow band of blocky material which is probably the downslope talus embayed by Pwr-d plains. The SW segment of the internal annulus consists of an arcuate plate made of COdf-a material which looks as it was first upthrusted southwestward and then embayed by the materials of Pwr-i and Pwr-d plains. At the western part of corona the Pwr-i plains

of the inter-annulus trough merge into the same plains as the region surrounding the corona. At the western margin of the corona annulus there is a group of three superposed and partly coalescing steep-sided domes. On the west the dome cluster is embayed by Pwr-d plains (Figure 15). On the east the cluster merges into a narrow strip of the small shields which also complicate the surface of one of the three domes (Figure 16). Further to the east is a strip of Pwr-i plains separated from the shield strip by a prominent slightly sinuous fault that makes stratigraphic relations between the dome cluster and Pwr-i unclear.

The corona core is a topographic dome surrounded by a circular trough mostly filled with Pwr-d, except for its southern segment the western part of which is occupied by Pwr-i while the eastern part contains younger plains (Pl-d) which embay both Pwr-i and Pwr-d (Figure 16). These plains are made of numerous mostly radar dark flows (Pl-d). The domical core consists of at least three varieties of materials: (1) Pwr-i; (2) fields of small shields (Psh) which appear partly fractured and embayed by Pwr-i and Pwr-d, and (3) densely fractured terrain with a roughly radial structural pattern which looks embayed both by Pwr-i and Psh and thus is evidently a correlative of COdf-a.

In the arcuate depression within the eastern segment of the annulus there is a locality of dark plains (Pda) with two small craters which are apparently sources of this material (Figure 15, 17). Relatively small (typically tens km across) patches of this type are seen outside the corona. Besides the presence of visible sources they are characterized by embayment of their material into neighboring local depressions including otherwise unobservable fractures and troughs. This gives the appearance of the patches as having finger-like margins, which was the basis for Head et al. (1992) to call them amoeboids. The apparently very high fluidity of the material of these plains (Pda) is evidence for relatively low viscosity.

In summary, the sequence of events whose signatures are seen at Aramaiti Corona Is the following:

(1) Emplacement of the COdf-a subunit of densely fractured materials and Its subsequent dense concentric faulting; this is the initial signature of corona activity. This material is evidently correlative with the Pdf unit and its fracturing was supposedly contemporaneous with the dense fracturing typical of the Pdf unit. In this area we have no direct evidence of the emplacement of the Pfr material although it is seen very close to the eastern segment of the Aramaiti annulus in the form of the previously described belt of fractured and ridged plains. The compressional deformation which formed broad ridges within the belt evidently influenced the oldest elements of the corona too; this is now seen in the form of the southwestward upthrusted plate of the COdf-a material of the SW segment of the inner annulus.

(2) Emplacement of shield fields (Psh) in the area of the corona core and its fracturing. Shield fields in the vicinity of Aramaiti outside the corona were probably emplaced at the same time but are typically not fractured subsequently.

(3) Emplacement of the lower subunit of the regional plains with wrinkle ridges (Pwr-i) and its involvement in the continuation of formation of the corona annulus

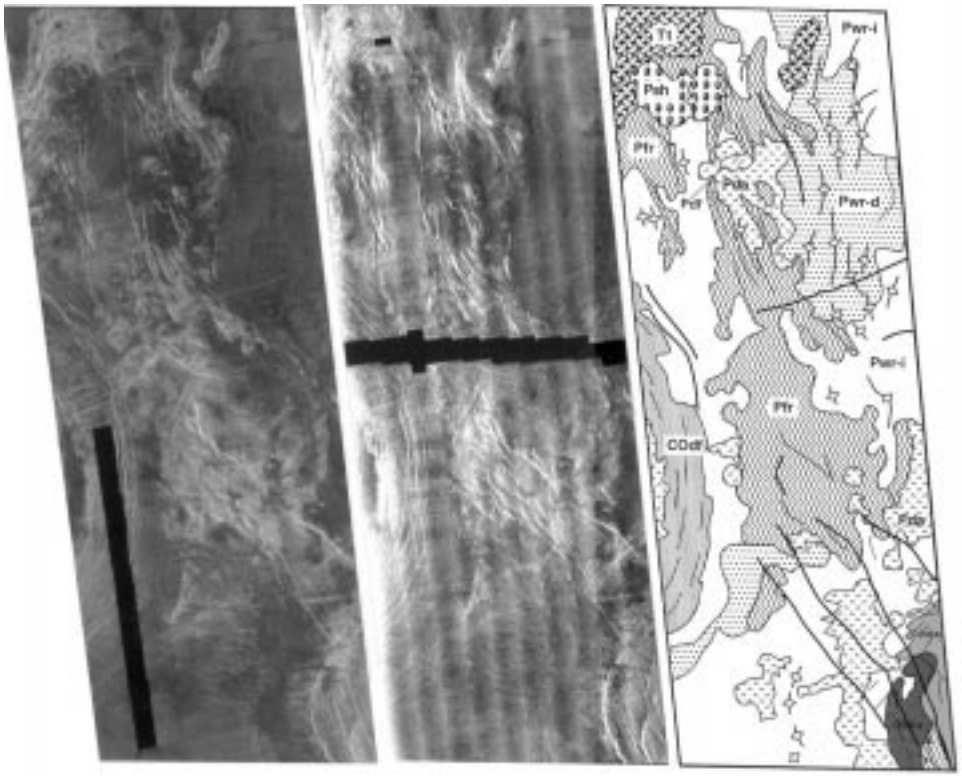

Figure 17. Stereopair of the eastern part of Aramaiti Corona (left), the Pfr belt, and the eastern part of Ohogetsu Corona (lower right); fragments of F-MIDRP-25S082;1 and F-MIDRP-25S082;301, with schematic geologic map of the imaged area; see text for unit designations. Area is 200 × 500 km.

(including concentric fracturing) and the trough in the northern part of the corona. At approximately the same time the troughs separating the corona annulus and core and outer and inner annulae in the corona north were formed.

(4) Emplacement of the younger subunit of the regional plains with wrinkle ridges (Pwr-d) including trough-filling. Plains emplacement was followed by emplacement of wrinkle ridges which deformed both Pwr-i and Pwr-d, and in some places Psh. The trend of wrinkle ridges is mostly near N-S, so they were not actively participating in the formation of the corona structure.

(5) Emplacement of patches of dark amoeboids (Pda) inside and outside the corona and emplacement of a patch of the dark lobate plains (Pl-d) south of the corona core dome. The latter is evidently the latest visible signature of the Aramaiti Corona activity.

It is important to note that easternmost part of the Aramaiti annulus (made of the COdf-b) is separated from the belt of Pfr plains deformed in broad ridges of probable compressional origin by a strip of the Pwr-i plains which is only 20 to 30 km wide (Figure 17). In spite of this closeness, no significant structural influence on

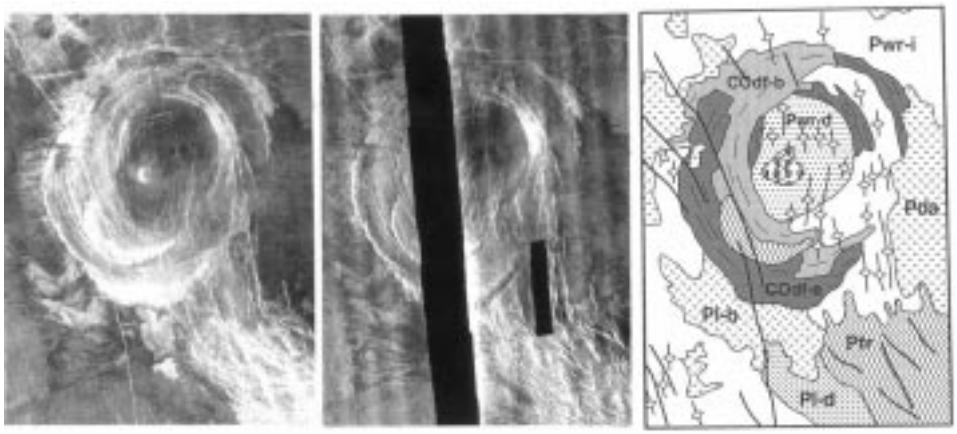

Figure 18. Stereopair of Ohogetsu Corona; fragments of C1-MIDRP-30S081;1 and C1-MIDRP-30S081;301, with schematic geologic map of the imaged area; see text for unit designations. Area is 280 × 350 km.

Aramaiti Corona from the regional compressional deformation that formed this Pfr belt is seen. One may conclude from this that at Aramaiti the COdf-b component of the corona started to form only after the formation of the belt, while the first signature of corona activity, in the form of the COdf-a component, predated the formation of the belt.

6. *Ohogetsu Corona:* (Concentric, 27.0°S, 85.7°E, D = 175 km): Ohogetsu Corona is adjacent to Aramaiti Corona, about 130 km to the SE, and these two coronae are separated by terrain composed of various plains units (Figures 1, 15, 18). The regional geologic setting for Ohogetsu is generally the same as for Aramaiti corona (Figure 15). The most important difference is that Aramaiti Corona is adjacent to the belt of Pfr plains with linear compressional ridges, while Ohogetsu is located on the strike of the belt between two linear belt segments. Examination of Figure 15a suggests that Ohogetsu is either superposed on the belt, or predated belt formation and its presence and characteristics were not influenced by the formation of the belt. Thus, this example provides an opportunity to assess the timing of corona formation relative to unit Pfr.

In the altimetry data (Figure 2) and in stereo, Ohogetsu corona shows a very variable hypsometric position along its annulus. In its eastern segment where it is in contact with the Pwr regional plains, the annulus stands only about 100 m above the plains. The northern segment of Ohogetsu is within a rise which is a part of the N-S trending belt which in most cases (but not here) is made of the Pfr unit. The summit of this rise is about 400–600 m over the surrounding plains and the northern sector of the annulus sitting in the south-looking slope of that rise is about 200–400 m over the plains. The eastern annulus of the corona is partly flooded by the younger plains whose surface is here by about 200–400 m below the normal level of the regional plains of this area. The southern segment

of the annulus, like the northern one, is on the slope of the N-S trending belt and it is about 100–200 m above the regional plains. The inner part of Ohogetsu is about 100–200 m below the level of the regional plains. The general impression is that Ohogetsu corona suffered significant deformation which disrupted its circular symmetry at least in the sense of its hypsometry. Ohogetsu Corona, like Aramaiti, has an annulus consisting of two varieties of densely fractured terrain (Figure 18). One of them, similar to the COdf-a subunit of Aramaiti, consists entirely of arcuate ridges and grooves separating them, all concentric to the corona structure. Another unit, an analog of COdf-b of Aramaiti, has a variable amount of plains-forming background cut by numerous concentric fractures. As in Aramaiti, the COdf-b subunit seems to be formed by fracturing of Pwr-i plains and embayed by Pwr-d plains, while the COdf-a subunit appears embayed both by Pwr-l and Pwr-d plains. The stratigraphically significant embayment of the COdf-a by the Pwr-i plains is best seen at 26.0°S, 87.0°E and 26.9°S, 84.8°E.

In the SW sector of Ohogetsu there is a peculiar arcuate feature. In stereo (Figure 18) it looks as a horse-shoe-shaped plate of relatively smooth plains upthrust over the middle part of the SW section of the annulus. The foot of the steep SW-facing slope of the scarp is in contact with the COdf-b subunit of the annulus. The concentric fracturing of COdf-b subunit here is truncated by this plate; this strengthens the impression that the feature is made by overthrusting. However the NE (downslope) part of this plate appears to be gradually changing into COdf-b material through the downslope increase in concentric fracturing of the plains of this plate. The interpretation of the upthrust, so clear at first glance, has two difficulties: (1) the fine concentric fracturing of COdf-b material looks unaffected at the place where the COdf-b material is supposedly upthrust by the plate; (2) the lateral (NW and SE) terminations of the horse-shoe-shaped plate do not show visible faults along which the supposed upthrust should occur.

These apparent conflicts may be understood if one assumes that (a) the upthrust predated the concentric fracturing of COdf-b or (b) even predated the emplacement of the Pwr-i material which the COdf-b material is apparently made of. In case (a) the plains-forming material of the plate might be the unfractured Pwr-i material. So the plate might be upthrust after Pwr-i emplacement but before the concentric fracturing occurred. However at that time the regional compression that formed the relatively broad ridges of the Pfr belt was already over while the compression forming wrinkle ridges superposed both on both Pwr-l and Pwr-d had not yet started. This evidence leads us to doubt case (a) and to favor case (b). In case (b) the plate material could be the unfractured and nonridged material of the Pfr plains whose upthrust was due to the event of regional compression which formed the Pfr belt with broad ridges.

The inner part of Ohogetsu Corona is occupied by dark Pwr-d plains deformed by a N-S trending set of wrinkle ridges extending southward Into the area of Pwr-i plains. Among the Pwr-d plains of the corona interior there is a shield about 10 km in diameter. Its age relations with the surrounding plains are not evident but

it looks to be an obstacle for the emplacement of wrinkle ridges so it evidently predated them, perhaps being part of unit Psh.

The eastern part of the Ohogetsu annulus is flooded by dark plains material which is very similar to the material of dark amoeboids (Pda) seen in Aramaiti Corona (Figures 15, 18). This material extends far southeastward off the corona and embays all the materials it is in contact with, including the younger unit of the plains with wrinkle ridges (Pwr-d) and the wrinkle ridges themselves. As seen in stereo, the locus of this material is within the flooded part of the corona annulus. Towards the SE the area of Pda material extends along the 350-km long flow of relatively bright lobate plains (Pl-b). To the west of that place, bordering the segment of the Pfr belt from its western side, there is another 350-km long flow of the lobate plains which differs from the first of the flows in that the plains are relatively dark (PI-d). These long P1-b and Pl-d flows are probably not associated with Ohogetsu corona activity, but have their sources within the prominent volcanic center at 34°S, 86°E. The SW rim of the corona Ohogetsu annulus is in contact with several shorter relatively bright flows probably associated with Ohogetsu activity.

In summary, the sequence of events observed in Ohogetsu corona is as follows:

(1) Emplacement of the COdf-a subunit of densely fractured materials and its subsequent dense concentric faulting. This material is evidently correlative with densely fractured plains (Pdf) and its fracturing was supposedly contemporaneous with the dense fracturing typical of Pdf. This event was the initial signature of Ohogetsu corona activity.

(2) Emplacement the material of the Pfr plains and its subsequent compressional deformation resulting in the upthrust of the largely pre-existing corona Ohogetsu and in its broad ridging elsewhere.

(3) Emplacement of shield fields (Psh).

(4) Emplacement of the lower subunit of regional plains with wrinkle ridges (Pwr-i) and its involvement in the continuation of formation of the corona annulus (including concentric fracturing) thus forming the COdf-b unit.

(5) Emplacement of the younger subunit of regional plains with wrinkle ridges (Pwr-d) including filling of the corona interior with these plains. This was followed by emplacement of wrinkle ridges which deformed both Pwr-i and Pwr-d and in some places Psh. The trend of wrinkle ridges is mostly N-S so they were not actively participating in the formation of the corona structure.

(6) Emplacement of the dark amoeboids (Pda) outside the corona and emplacement of the dark (P1-d) and bright (P1-b) lobate plains SW and SE of the corona. Some of these deposits (Pda) may be associated with the late stages of Ohogetsu evolution.

Cross-correlation of Corona-forming Activity with Local, Regional, and Global Stratigraphy

Regional and Global Stratigraphy Model		Verdandi		Thourus		Belet-ili		Gaya		Aramaiti		Ohogetsu	
		1	2	1	2	1	2	1	2	1	2	1	2
Aurelia	Cdp												
Atla	Pl, Ps			P	V					P	V	P	V
Rusalka	Pwr, Psh	P		P	WR?	P	WR	P	WR	P	CF	P	CF
Lavinia	Pfr, RB			P		P						P	
Sigrun	Pdf	P	CF	P	CF	P	CF	P	RF	P	CF,RF	P	CF
Fortuna	Tt	P				P							

1 - Local stratigraphic column; 2 - Corona-forming and corona-related activity;
P - The unit is present; CF - Concentric fracturing; RF - Radial fracturing;
WR - Wrinkle ridging; V - indigenous activity.

Figure 19. Cross-correlation of corona-forming activity with local, regional, and global stratigraphy. (1) local stratigraphic column; (2) corona-forming and corona-related activity; P, the unit is observed; CF, concentric fracturing; RF, radial fracturing; WR, wrinkle ridging; V, volcanic activity.

4. Discussion

1. *Stratigraphic Units and Structural Features:* Analysis of the stereo images of the six coronae described above shows that the geology of each of them can be characterized in terms of a specific set of material complexes (stratigraphic units) and structural elements deforming or not deforming them. These complexes either are units identified in the model of regional and global stratigraphy of Venus (Basilevsky and Head, 1995a–c; Basilevsky et al., 1997a) or are specific to coronae, but are correlative with the regional and global units. These data now give us the possibility to consider the first of the questions formulated in the Introduction: "When in the local, regional, and global stratigraphic context, did different coronae start to form and when did their evolution cease?"

In our previous studies we found that tessera material and tessera-forming deformation predated all corona-forming materials and structures (Basilevsky and Head, 1995a–c). This study supports this conclusion: In two of six cases tessera terrain was observed so closely neighboring the coronae that through analysis of their relations it was possible to conclude that the tessera-forming material and deformation predated the emplacement of the most ancient corona-forming material and deformation (Figure 19).

From the descriptions given above it follows that for all six coronae the most ancient component of their annulae Is COdf or COdf-a materials correlative with the material of densely fractured plains (Pdf). In all these cases the Pdf-type mate-

rial forms inliers standing above the regional Pwr plains that are embaying them. It is clear that deformation of this material to form COdf represents the now-distinguishable beginning of formation of the corona structure. It is not clear whether the emplacement of this material was related to the corona formation process (for example, volcanism fed by a plume whose upwelling might have initiated the corona-forming deformation) or if this material is part of the regional plains materials present at that time (for example, the source of the volcanism was not related to the corona-forming process). Because inliers of Pdf material are often observed without any visible association with coronae, we believe that the second option is more likely. If this is true, then one may conclude that the first phase of corona formation was a tectonic phase.

As in the majority of other regions of Venus, in the areas of the six coronae we studied, the most abundant unit is material of Pwr plains. This unit surrounds the coronae, dominates within corona interiors, and in four of six cases (Belet-ili, Gaya, Aramaiti, Ohogetsu), Pwr forms the dominant part of their annulae. This Pwr material within these coronae appears similar to Pwr material in close regional association with the coronae and also to that at much greater distances (e.g., Basilevsky and Head, 1995a–c). Both inside and outside the coronae the sources of this material are not readily observed, a situation that is also similar for the majority of regional volcanic plains on the Moon (Wihelms, 1987) and Mars (Tanaka et al., 1992). On the Moon, some of these plains are associated with extensive sinuous rilles (Carr, 1973) and channels (Schaber, 1973), both suggestive of high effusion rates (Head and Wilson, 1992), and similar to channels and canali observed in the venusian plains with wrinkle ridges (Baker et al., 1992). These data suggest that the regional plains with wrinkle ridges formed from relatively high effusion rate eruptions that were different in style from that characterizing most units preceding and postdating it (Head et al., 1996), The Pwr-forming eruptions were probably not related to the corona-forming plumes because many plains of this type are observed on Venus without any visible association with coronae. In four of the six mapped coronae, only one variety of Pwr material was distinguished and mapped. In two cases (Aramaiti and Ohogetsu) two varieties of Pwr material were observed. The earlier unit, (Pwr-l), was involved in corona-forming deformation, thus producing the COdf-b unit, while the later one (Pwr-d) buried the depressions inside and outside the coronae and was not involved in the corona-forming deformation.

The orientation of wrinkle ridges (which are characteristics of Pwr plains) in three of six cases (Verdandi, Aramaiti, Ohogetsu) is not in alignment with the corona structure. Within and in close proximity to the coronae the orientation is the same as it is at greater distances. In one case (Thourus), a portion of the wrinkle ridge set approaching the corona changes orientation slightly toward a radial trend. In two cases (Belet-ili and Gaya), wrinkle ridges deforming Pwr material are the most significant of the observed structural components of these coronae, strongly suggesting that these two coronae were extensively flooded by Pwr plains and that subsequent corona-forming deformation continued to produce prominent

deformation of the emplaced plains. It is interesting that the most topographically prominent corona studied (Verdandi) lacks wrinkle ridge alignment with the corona structure, while coronae Belet-ili and Gaya, which are essentially indistinguishable in topographic prominence from the other three coronae (Thourus, Aramaiti, Ohogetsu), have annulae that are comprised mostly of wrinkle ridge arcs. We interpret this to mean that orientation of wrinkle ridges within and in the close vicinity of the coronae was controlled by local corona-related stress but not a passive load of corona topography. But this is certainly not the case for Aramaiti and Ohogetsu, where pre-wrinkle-ridge formation of the topography is indicated by the localization of the later Pwr units (Pwr-d) in the presently observed lows. We also interpret this to mean that at the time of wrinkle ridge formation, the evolution of Verdandi, Aramaiti and Ohogetsu coronae had ceased, the evolution of Thourus corona was essentially over, and that Belet-ili and Gaya coronae were still tectonically active.

Volcanic flows obviously associated with coronae were observed in only three cases (Thourus, Aramaiti, Ohogetsu) and these flows postdated wrinkle ridge formation. In Thourus and Aramaiti this later volcanism was localized within the corona interior. Ohogetsu corona lacks the later interior volcanism but has an anomalously large area of amoeboid material (Pda) in association with its SE margin. On the basis of these observations we conclude that three of the six coronae studied had a volcanic phase in their evolution which postdated the tectonic phase. For the other three coronae, only the tectonic phase of their evolution is observed (Figure 16). The degree of preservation of earlier corona-related activities and the scale of later corona-related activities vary significantly from corona to corona.

It is worthwhile to compare the results of this analysis with studies of coronae in other regions in order to see if the trends are similar. Basilevsky and Head (1994, 1995a–c) described the geology and stratigraphy of thirty-six 1000 $\times$ 1000 km areas in which 48 coronae and corona-like features were observed; descriptions of these coronae can be found in these publications. Of that sample, 33 coronae have an annulus partly or completely made up of Pdf/COdf material. About half of these have in their annulae (in addition to Pdf material) material deformed by wrinkle ridges (mostly Pwr plains) and sometimes deformed by broad ridges (Pfr material). In a few cases coronae were identified only due to the presence of an annulus made of wrinkle ridges; typically these are relatively small structures of the arachnoid type (150–200 km in diameter) (Barsukov et al., 1986; Nikishin et al., 1992; Head et al., 1992). In three of the thirty-six areas, coronae outlined only by concentric fractures younger than Pwr plains were observed. Young post-Pwr material of lobate plains (P1) was observed in association with 22 coronae. In two of those thirty-six areas these young corona-associated lobate plains are crossed by even younger concentric fractures which partly or completely outline the corona structure.

On the whole the results of Basilevsky and Head (1994, 1995a–c) are in agreement with the present results of the analysis of the six coronae. For example, in their sample of over 45 coronae, the earliest corona-forming deformation cuts Pdf/COdf

material. About half of the corona of this sample were tectonically active during wrinkle ridge formation. A volcanic phase of coronae evolution was found to occur only in some of the coronae and it was represented by emplacement of relatively young (post-Pwr) lavas. Only rare cases of corona-associated and even corona-forming deformation contemporaraneous with the volcanic phase (or even later) were observed.

Jackson et al. (1996) studied the geology of Bell Regio, including Nefertiti corona (36.0°N, 49.0°E, 225 × 500 km) situated in its northern part. According to their description, the majority of the corona annulus consists of two generations of material of densely fractured terrain appearing similar to Pfr/COdf material of Basilevsky and Head (1995a–c). The eastern part of the annulus is represented by an arcuate cluster of broad ridges made of material appearing similar to units Pfr/RB. In addition, at the western edge of the corona there are wrinkle ridges organized in a pattern concentric with the corona structure. Jackson et al. (1996) believe that these wrinkle ridges may be younger that the regional network of wrinkle ridges observed in this area. An apron of lobate flows is seen emanating westward of the corona annulus. In their opinion, these flows appear to overlap the regional Pwr plains and are deformed by the concentric system of wrinkle ridges.

Jackson et al. (1996) describe two options for correlation of the corona-forming and corona-associated units with regional and global stratigraphic units. In the first option, material of the densely fractured terrain and broadly ridged terrain in the Nefertiti annulus is older than the regional Pwr plains; this would imply that the majority of the corona components formed mostly in pre-Pwr time. In the second option, all structural elements in the Nefertiti annulus are the result of deformation of regional Pwr plains. Both of these options have analogs among the six coronae we studied. The first option resembles the situation observed in Thourus corona. The second option resembles the evolution of Aramaiti and Ohogetsu coronae after the emplacement of Pwr-i material. In addition, Jackson et al. (1996) show that Nefertiti corona had a prominent volcanic phase in its evolution which started either in post-Pwr time (if the concentric wrinkle ridges postdate the wrinkle ridges of the regional network) or at some time before the emplacement of the regional wrinkle ridge network (if the concentric wrinkle ridges are part of the regional wrinkle ridge network).

Pronin (1997) recently published the results of a photogeologic and mapping analysis of thirty coronae. Unfortunately for comparison to the analysis of stratigraphic position of different phases of coronae evolution, Pronin (1997) mapped only four of them with reference to stratigraphy, and the majority of them were mapped only from a structural, not a stratigraphic/structural standpoint. Of the four mapped by Pronin (1997), one is Gaya corona, mapped also in our study. The results of the mapping of this corona by Pronin (1997) and in our study are practically the same: the corona annulus is represented by a ring of wrinkle ridges deforming Pwr-plains material and inside are remnants of the corona core made of COdf/Pdf material deformed in a radial pattern.

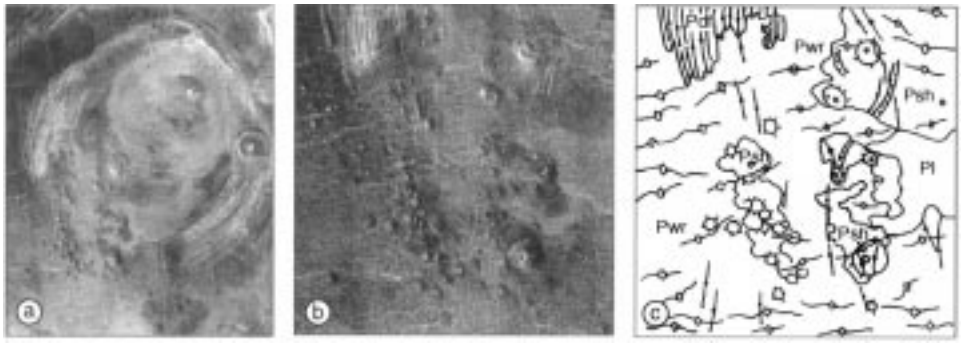

Figure 20. Plains with shields in the SW largely flooded part of the annulus of Allatu Corona. (a) Magellan image of Allatu Corona (portion of F-MIDRP-15N111;1). Area 150 km wide. (b) SW portion of Allatu Corona (portion of F-MIDRP-15N111;1). (c) Geologic sketch map of area in middle showing early densely fractured plains forming a remnant of the corona annulus (COdf), shield plains (Psh) which are cut by graben, both of which are then flooded by regional plains with wrinkle ridges (Pwr) and lobate plains (Pl). The latter are probably a part of the corona-related activity. Note kipukas of shield volcanoes decreasing in abundance in distance away from the embayed Psh units. Area is 85×80 km.

The remaining three coronae mapped stratigraphically by Pronin (1997) have not been analyzed by us either in this study or previously. One of these is the 150-km corona Allatu, located in Niobe Planitia. Its annulus is made of material of densely fractured terrain evidently correlative with Pdf/COdf material. The annulus is embayed by material of typical Pwr plains. The wrinkle ridges deforming this material are not in alignment with the corona structure. In the corona vicinity there are patches of plains- forming material which was considered by Pronin (1997) as an older subunit of Pwr plains (Pwr-old): it is embayed by the dominant component of Pwr plains. We studied images of this area and found that immediately north of the area studied by Pronin (1997) there are patches of the same material deformed by broad ridges typical of our Pfr/RB plains. Inside the corona annulus are mapped younger plains, correlative to our Pl/Ps plains, and volcanic shields of the Psh type which according to interpretation of Pronin (1997) are part of this corona-related volcanic suite.

We analyzed Magellan images of Allatu corona and confirmed the presence of young volcanic plains in association with this corona. However, we disagree with the interpretation (Pronin, 1997) that the Psh-type volcanic shield plains are a signature of young corona-related volcanic activity. Instead, our analysis (Figure 17) found that these shields are quite abundant in this region both regionally (without association with any coronae) and in areal association with Allatu and other coronae. Moreover, most of these shields including those within Allatu, show evidence of embayment by the regional plains with wrinkle ridges (Pwr) (Figure 20). So these shields are clearly not a part of the late Allatu corona-related volcanism but a signature of older volcanic activity of regional significance.

The second of those four coronae is an arachnoid (150 × 250 km in diameter) centered at 42.5°, 214.3°E. Its annulus is made of Pwr plains deformed in a radial-concentric pattern. Inside and outside the corona annulus there are patches of young smooth plains evidently correlative to our Ps plains. It is not clear if the younger plains are associated with the corona or are part of more regional plains.

About 150 km southwest of this arachnoid, Pronin (1997) mapped an unnamed 150-km corona (40.5°N, 212.3°E). Its annulus is made of material of densely fractured terrain correlative with our COdf/Pdf unit. It is embayed by typical Pwr plains. Inside the corona wrinkle ridges deforming this material are in alignment with the corona structure. Corona-associated young volcanics correlative with our Pl/PS plains are also mapped.

In summary, joint consideration of the results of the study of six coronae described in this work and of earlier published results on about thirty other coronae allows us to answer the first of questions formulated in the Introduction ("When in the local, regional, and global stratigraphic context, did different coronae start to form and when did their evolution cease?") in the following way: The majority of the coronae considered started to form as a result of concentric/radial deformation of the material correlative with the Pdf unit before the emplacement of the material of the regional and global Pfr/RB unit. For about half of these coronae this deformation was the only visible tectonic episode of corona-forming activity and later they only passively withstood regional tectonic and volcanic events. An additional half of the coronae were still active tectonically during the time of emplacement of the regional wrinkle ridge network. This evolutionary stage added to the corona annulae arcs of wrinkle ridges and for some of them it produced their entire visible (wrinkle ridge) annulus. In rare cases the corona-related tectonic deformation continued or occurred after the emplacement of the regional wrinkle ridges and, in even rarer cases, after emplacement of at least some of the lobate and smooth plains (Pl/Ps), thus adding concentric and radial fractures to already existing corona structure or, very rarely, producing the entire now-visible corona annulus. In summary, the tectonic deformation stage of the corona population seemed to have its peak in Pdf time (Sigrunian), was decreasing in Lavinian and Rusalkan time, and was almost completely terminated by Atlian (Pl/Ps) time.

Obvious corona-related volcanic activity is observed only in about half of the coronae considered in these studies. This volcanism occurred mostly in the form of emplacement of Pl/Ps plains of Atlian age. In rarer cases it occurs in the form of a late subunit of Rusalkian Pwr plains, or both. No evident correlation exists between the presence of volcanic activity and the longevity of corona tectonic deformation in the subpopulation of coronae we studied. There are a few examples of coronae in which volcanic activity, which is typically young, is associated with relatively young tectonic activity. But the commonest cases are those where there was a significant apparent stratigraphic gap (from Sigrunian (Pdf) to Atlian (Pl)) between tectonic and volcanic phases of the corona evolution.

2. The second question formulated in the Introduction: “Did coronae evolution occur synchronously in the sense that the same type components of different coronae formed at approximately the same time or, alternatively, that the evolution of each corona was absolutely not correlated in time with the evolution of other coronae?” can be answered in detail only if reliable regional and global stratigraphic correlations with synchronous planet-wide stratigraphic markers are available. As previously mentioned, such a stratigraphy (Basilevsky and Head, 1995a–c; Basilevsky et al., 1997a,b) is only a model which is now undergoing tests at various scales. Several lines of evidence supporting its main features were discussed above, but further tests of the model are beyond the scope of this paper. In this discussion we will try to answer the second question using two approaches: (1) assuming that the model is correct, and (2) without any assumptions, and simply considering the stages of evolution of coronae which are so close in proximity that the synchroneity of the same geologic units between them is obvious.

(1) Let us assume, first, that the model is correct. In that case the conclusions reached above (that several components of the mapped coronae are correlative with the appropriate units of the regional and global stratigraphic scheme) means that the components of the same type observed in different coronae did form at approximately the same time.

(2) Second, we consider cases when two or more coronae are so close in proximity that synchroneity of some of the regional geologic units between them is obvious. Among the six coronae studied in this work there are two such pairs: a) Belet-ili and Gaya and b) Aramaiti and Ohogetsu.

Belet-ili and Gaya are touching each other (Figure 10a) and the outer part of the NW segment of the Gaya annulus is actually the southern part of the Belet-ili annulus. No evidence of superposition of one of these coronae on the other one is seen, so emplacement of the wrinkle-ridge-forming annulus of one of these coronae was obviously contemporaneous with emplacement of the wrinkle-ridge-forming annulus of the other one. The vast majority of the material of Pwr plains deformed by these wrinkle ridges appears on the images to be similar, with no visible contacts in the area of transition from one corona to another, giving the impression of continuity of this material in this place. So, at least in relation to the final stages of evolution of neighboring Belet-ili and Gaya, the observations show that components of the same type formed in these two coronae at the approximately the same time.

Aramaiti and Ohogetsu (Figure 15a) are separated by only 150 km of Pwr-i plains material with inclusions of patches of Pwr-d and Pda. The continuity of unit Pwr-i in the transition zone between Aramaiti and Ohogetsu appears clear and it seems reasonable to consider unit Pwr-i as a stratigraphic bridge between the stratigraphic columns of these coronae.

The two columns show very good correlation of units between them: Pdf and its early concentric fracturing are at the base of both columns, followed by Psh and Pwr-i, then another episode of concentric fracturing followed by episodes of

emplacement of unit Pwr-d and subsequent wrinkle ridging of both Pwr units, and finally on top of both columns there is a suite of amoeboid plains (Pda) and lobate plains (Pl-d, Pl-b). The Pwr-i bridge correlates these two columns but, of course, its constraint on synchroneity of similar units of these two columns weakens stratigraphically upward and downward from the bridge itself. Fortunately there is one more tool to correlate these columns. This is the episode of E-W compression which is interpreted to form the Pfr/RB ridge belt of this area, the horse-shoe feature in corona Ohogetsu, and the upthrust of the SW segment of the inner annulus of Aramaiti. If the previously described interpretations of the formation of these three features are correct, this episode of compressional deformation is another stratigraphic bridge which strengthens the point of approximate contemporaneity of Pdf-a units of these coronae. Thus, consideration of the geology of the neighboring coronae Aramaiti and Ohogetsu shows that their individual components of the same type formed at approximately the same time.

In summary, the tentative answer to the second question is: On the basis of our sample, we interpret the evolution of many coronae to have occurred quasi-synchronously in the sense that the same components (units and structures) of different coronae formed at approximately the same time.

3. To address the question concerning the absolute time duration of formation and evolution of individual coronae and what was the time duration since the beginning of formation of the corona population until its termination, we may use three approaches: (1) estimates based on crater counts on coronae and other terrains on Venus; (2) estimates based on theoretical models of corona formation; and (3) lifetime durations of features thought to be analogous, such as terrestrial hot-spot structures.

(1) Attempts to estimate the absolute age of coronae were made by Namiki and Solomon (1994) and Price and Suppe (1994). Because of the limited number of craters and the relatively small area of the individual coronae, these estimates are mean values for the total corona population, or, at the best, for some categories of them. These works compare crater densities with the global average, well determined as about 2 craters per million km^2 (Schaber et al., 1992; Phillips et al., 1992), and consider their age estimates in terms of global average age T. The latter is subject to large uncertainties, mostly related to uncertainties in the assumed rate of the collision of the crater-forming projectiles with Venus: Strom et al. (1994) estimated the average crater age of Venus as 288 + 311/−98 m.y. (usually considered as about 300 m.y. for convenience). Phillips et al. (1992) estimated the global average surface age in the range 400–800 m.y. (about 500 m.y. is adopted for convenience). Recently Zahnle and McKinnon (1996) reconsidered the crater production rate on Venus and estimated the global average surface age of that planet as 800 m.y. (possible range of 400–1600 m.y.). Thus, besides the statistical uncertainties due to the small number of craters on the coronae, all the following estimates also have the uncertainty of estimation of T which, unfortunately, is within a factor of 3 or so.

Namiki and Solomon (1994) used the corona data base of Stofan et al. (1992) and determined the crater density inside the outer boundary of the corona annulae. They divided 358 coronae under study into five groups reflecting their evolutionary stage. For the three groups which include coronae with a predominance of features corresponding to the earlier stages of evolution, the crater density and therefore the surface age are found to be indistinguishable from the global average. For coronae of the so-called categories 2 and 3, with a significant amount of associated intra-corona volcanism, the crater density ($-1+/-0.5$ craters per million km^2) is about one-half of the global average. Averaging crater counts for all coronae Namiki and Solomon (1994) obtained a crater density of about 0.7 of the global. So the average age of coronae is $-0.7T$ and average age of coronae with a significant amount of late volcanism is $-0.5T$, where T is the average surface age of Venus.

Price and Suppe (1994) estimated the average crater density for 364 coronae as $1.12+/-0.34$ craters per million km^2, thus generally confirming the results of Namiki and Solomon (1994). Making a correction for the possible presence of pre-corona craters in this crater subpopulation Price and Suppe estimated the average age of the coronae as $0.28+/-0.37T$.

As exemplified by the stratigraphic work presented here, we should keep in mind that coronae are typically the products of multistage tectonic and volcanic activity represented by units from Pdf/Pfr through Pwr/Psh to Pl/Ps. This of course means that these estimates refer to a mixture of all those units, with stronger statistical weight for the Pwr-PI/Ps units. What estimates of surface age do exist for different units involved in corona formation?

The Pdf and Pfr units, the most ancient for coronae, have relatively small areas so their average surface age cannot be reliably estimated through crater counts. The tessera terrain material (Tt) underlying them has a larger areal abundance and was analyzed in terms of crater counts. The total crater density on the Tt unit was found to be close to the global average (Ivanov and Basilevsky, 1993; Strom et al., 1994). However, on tessera the smaller (<16 km in diameter) craters have a lower density than the global average of craters of that size, while the larger on-tessera craters have a density higher than the appropriate global average. If we consider the lower density of the smaller on-tessera craters as an observational effect and rely on the density of relatively large craters, the estimated average tessera age Is $1.47+/-0.46T$ (Ivanov and Basilevsky, 1993).

Pwr plains with inclusions of Psh dominate in many coronae in terms of areal abundance; they also comprise the majority of the surface of Venus (Basilevsky et al., 1997b; Ivanov and Head, 1997a,b). The distribution of craters on the surface of Venus is indistinguishable from random (Schaber et al., 1992; Phillips et al., 1992) and this means that the crater density on the Pwr/Psh complex Is very close to the global average. This is confirmed by the estimate of Price and Suppe (1994) who found that the crater density on their plains unit (which is apparently what we call the combined Pwr/Psh plains) is indistinguishable from the global average. So the average surface age of Pwr/Psh plains should be very close to T. Because the great

majority of impact craters superposed on Pwr plains are also superposed on the wrinkle ridges deforming these plains (Strom et al., 1994; Basilevsky, 1996b), the emplacement of the wrinkle ridge network can be dated also as $\sim T$.

Younger Pl/Ps plains, abundant in many coronae, are even more abundant in association with rift zones where they are present in the form of lava flows composing large volcanoes and plains-forming lava fields (Magee and Head, 1993; Magee and Head, 1995). Namiki and Solomon (1994) estimated the crater density on 175 volcanoes at least 50 km in diameter to be 0.9+/−0.2 craters per million km^2; this is about half the global average. Price and Suppe (1994) studied crater densities on 128 large volcanoes and found there to be 0.51+/−0.32 craters per million km^2. The difference from the results of Namiki and Solomon (1994) is probably due to the somewhat different volcano population studied by these research groups and to the stochastic nature of the cratering process. Price and Suppe (1994) also estimated the crater density on a composite sample of 48 flood-type lava flow fields. The majority of them are apparently what we call Pl plains, but some lobate plains of the younger Pwr subunit(s) may be also present among the studied lava fields. The average crater density on these 48 lava fields was found to be 0.92+/−0.65 craters per million km^2. Combining the estimates for large volcanoes and lava fields leads to an estimation of their average surface age as close to $0.5T$. Because some lavas of this suite are probably younger than $0.1T$ (Basilevsky, 1993), in order to have the average age of the entire suite $\sim 0.5T$, some members of it should be noticeably older than $0.5T$.

In summary, this consideration shows that the majority of the coronae considered started to form at the time period between $\sim 1.5T$ and $\sim 1T$. At the time period close to T about half of them were already tectonically inactive, but another half were still tectonically alive. At the time soon after about T (after the episode of wrinkle ridging), the majority of the coronae considered were tectonically dead. The volcanic phase, whose signatures are observed for about half of the coronae considered, occurred at the time period in between $1T$ and $0.5T$, probably with some cases of corona-related volcanic activity slightly older than $1T$ and some case of volcanic activity younger than $0.5T$. If we assume, as many authors do, that T = 300 m.y., for the majority of the coronae considered, the starting time was between 300–450 m.y. ago and their activity ended between 150 –300 m.y. ago. The volcanic phase of the corona activity is even less constrained: it occupies an unknown duration somewhere in between $1T$ and $0.5T$. Although it is not very certain information, it nevertheless shows that the lifetime of typical coronae was of the range of tens to a few hundred million years and the lifetime of the total population might be as long as a few hundred million years.

(2) Terrestrial hot spots are believed to be a result of upwelling of mantle plumes and in this respect they certainly are kindred to the venusian coronae independently of the question of whether venusian mantle plumes originated in the same part(s) of the interior as did terrestrial hot-spot-forming plumes. There are at least two partly overlapping kinds of terrestrial features formed by plumes: (a) classical hot spots

exemplified by the Hawaian-Emperor chain in the Pacific or Hoggar in Africa, and (b) the flood basalts areas exemplified by the Columbia River basalts in North America or Siberian traps in Northeast Asia. The lifetime of the first type is found to be not more than ∼70 m.y. (Condie, 1989) or about 100 m.y. (Hess, 1989). The lifetime of the second type varies from about 10 m.y. to about 30–40 m.y. (BVSP, 1981; Tolan et al., 1989; Brewer et al., 1992). These are estimates of the lifespans of plume-associated volcanic events so they should be considered for comparisons with the lifespans of the volcanic phase of the venusian coronae.

(3) Theoretical models consider the formation of coronae as a result of the rise of mantle plumes, their impinging on the underside of the lithosphere, causing topographic uplift, producing radial spreading, flattening and subsequent cooling, thus removing the thermal support and allowing gravitational relaxation of the topographic bulge. Calculations show that this process requires about 100–200 m.y., about one-half of which is the time of the plume emplacement and the existence of its thermal anomaly (see, for example, Smrekar and Stofan, 1996; Smrekar and Parmentier, 1996; Janes and Squyres, 1995). Melting which may produce the observed corona-related volcanism is predicted to start about 40 m.y. after the plume encounters the lithosphere (Smrekar and Parmentier, 1996). Other models estimate ranges from 10–20 to 200 m.y. depending on variations in mantle viscosity, but favor 30–50 m.y. (Musser and Squyres, 1997). This is in general accord with earlier estimations of the timing of terrestrial mantle plume upwelling which predicts in particular that the surface uplift preceded the mantle-associated volcanism by about 3 –30 m.y. (Griffiths and Campbell, 1991; Hill et al., 1992).

Thus, joint consideration of the results of the study of six coronae described in this work and of earlier published results on about thirty other coronae gives us the possibility to construct a scenario for the formation of venusian coronae (Figure 21). The majority of the coronae considered started to form in Sigrunian time with the corona-forming deformation of the Sigrunian materials which probably were the products of the regional plains of that time. A minority of the coronae considered, namely those whose most ancient components are younger than the Pdf unit, could also start to form in Sigrunian time and be covered by later deposits, but we have no positive evidence for that; thus, this minority could also start to form after Sigrunian time. About half of the coronae considered ceased their recognizable tectonic life during the Lavinian and Rusalkan times, but another half were tectonically active during the end of the Rusalkan time when the emplacement of the regional wrinkle ridge network occurred. For many coronae this Rusalkan evolutionary stage added arcs of wrinkle ridges to their annulae following their burial by plains with wrinkle ridges. (Pwr). For some it produced all their visible annulae in the same manner. In rare cases, corona-related tectonic deformation continued into Atlian time, either adding relative minor concentric and radial fractures to already existing corona structure or, in even more rare cases, producing the whole presently visible evidence of the buried corona annulus. Finally,

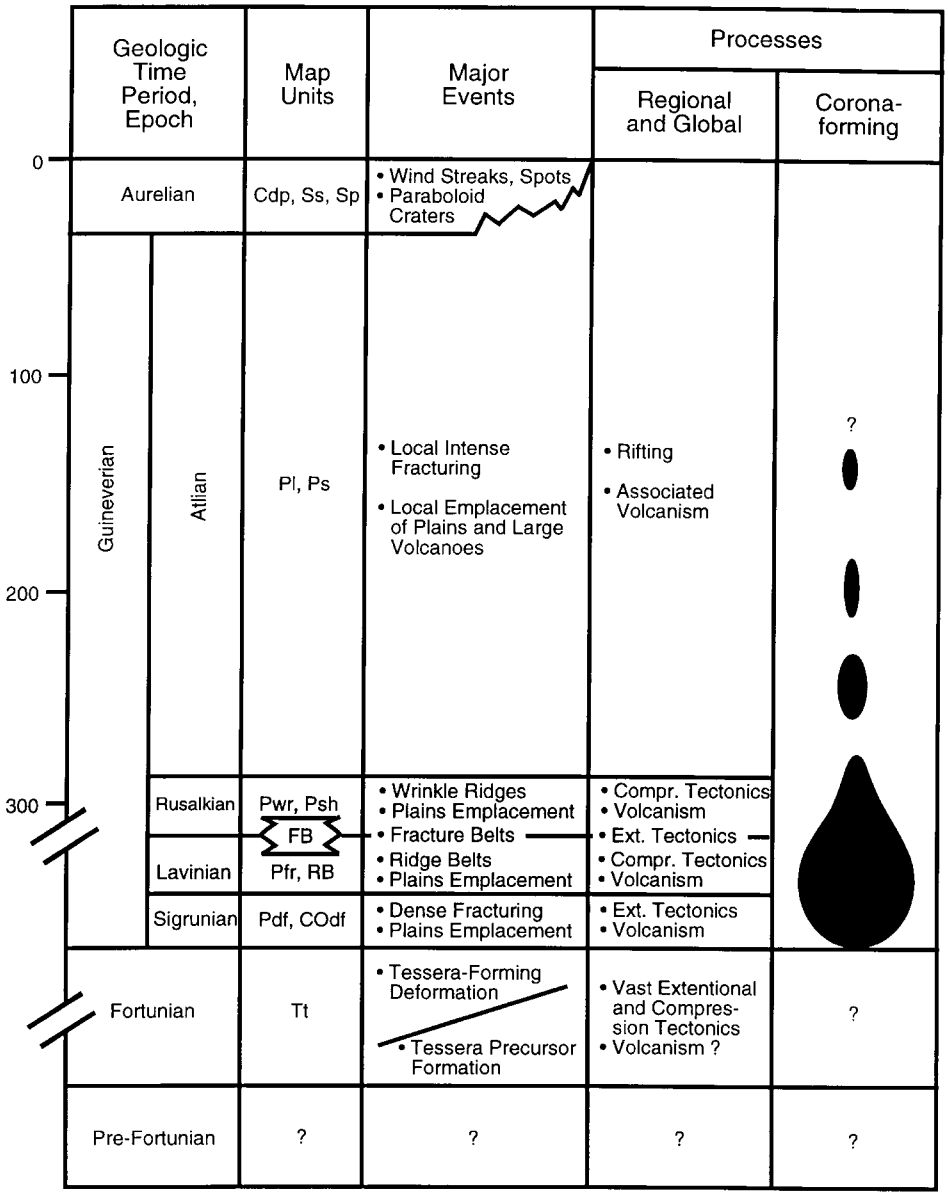

Figure 21. Summary of Venus global stratigraphy and geologic history. For convenience the global average surface age is considered to be 300 m.y.

topographic subsidence continued for some coronae into this period, as shown by interior topographic depressions formed of warped Pwr units.

Volcanic eruptions specifically associated with coronae (as distinguished from regional plains) started in some coronae about the end of Rusalkan time, and in the majority of coronae having a volcanic phase, during Atlian time. This volcanic

activity lasted through an unknown part of the Atlian time. If we apply to coronae the estimations of timespans found from terrestrial hot spot studies and from theoretical modelling, one may suggest that the timespan between the early Sigrunian deformation (the plume had started to impinge the lithosphere) and the beginning of the corona-related Atlian volcanism was as large as a few millions to a few tens of millions years. This is in general agreement with estimation of Collins et al. (1997) that the timescale of emplacement of plains with wrinkle ridges – which is a part of the considered timespan – was about 5 –30 m.y. Based on the analogy with terrestrial hot spots the corona-related Atlian volcanism could have lasted for about a hundred million years.

5. Conclusions

This study supports the observations made earlier by us (Basilevsky and Head, 1995a–c, 1997b; Basilevsky, 1995) and others (e.g., Stofan et al., 1992; Pronin, 1997) that coronae formed by multi-stage tectonic and volcanic activity. In addition, our study demonstrates that these stages are manifested in a typical sequence of geologic units and structures and that these stages occupy very specific positions in the regional and global stratigraphic column. The units and structures of similar morphology seem to be quasi-synchronous around the planet.

In the sample analyzed, coronae formed in a two stage process; the first stage (tectonic phase) involved the annular warping of early extensive stratigraphic units of volcanic origin and the second (volcanic phase) involved coronae-related lava flow activity and local fracturing. For the vast majority of coronae, the first tectonic phase was largely complete prior to the emplacement of the regional plains (Pwr, plains with wrinkle ridges). The vast majority of corona-related volcanic activity (emplacement of Pl, lobate flows) occurred subsequent to the emplacement of regional plains. We found no evidence of coronae initiation in substantially later periods of the observed history of Venus.

In summary, our observations show that soon after the cessation of tessera formation there was a massive initiation of corona formation, and with time, corona-forming activity decreased significantly and maybe even ceased completely in geologically recent time (Figure 21). This may be due either to a decrease in the rate of generation of the corona-forming mantle plumes or to decreasing ability of the plumes to form coronae, for example due to thickening of the lithosphere with time, or both. Alternatively, coronae could represent a stage in the evolution of Venus in which thermal evolution created instabilities in the mantle resulting in widespread coronae formation (e.g., Parmentier and Hess, 1992; Head et al., 1994). This information on the sequence of events and apparent near-synchroneity of aspects of coronae formation should be useful for distinguishing among geophysical models for coronae development and the general geophysical evolution of Venus.

Acknowledgments

We gratefully acknowledge the assistance of the following individuals; M. A. Ivanov, V. P. Kryuchkov, and A. A. Pronin for constructive discussions of issues considered in this paper; Peter Neivert for photographic support; Paul Haggerty for computer support; Anne Côté for drafting. Partial financial support was provided by the Planetary Geology and Geophysics Program of NASA in the form of NASA Grant NAGW-1873 to JWH.

References

Aubele, J. C.: 1995, 'Stratigraphy of Small Volcanoes and Plain Terrains in Vellamo Planitia – Shimti Tessera Region, Venus', *Lunar Planet. Sci.* **26**, 59–60.

Aubele, J. C.: 1996, 'Akkruva Small Shield Plains: Definition of a Significant Regional Plains Unit on Venus', *Lunar Planet. Sci.* **27**, 49–50.

Baer, G., Schubert, G., Bindshadler, D., and Stofan, E.: 1994, 'Spatial and Temporal Relations between Coronae and Extustional Belts, Western Lada Terra, Venus', *J. Geophys. Res.* **99**, 8355–8369.

Baker, V. R., Komatsu, G., Parker, T. J., Gulick, V. C, Kargel, J. S., and Lewis, J. S.: 1992, 'Channels and Valleys on Venus: Preliminary Analysis of Magellan Data', *J. Geophys. Res.*. **97**, 13,421–13,444.

Barsukov, V. L. et. a.: 1984, 'Geology of Venus from the Results of Radar Images Received by Venera 15 and 16 Probes: Preliminary Data (in Russian)', *Geokhimia* **12**, 1811–1820.

Barsukov, V. L. et. al.: 1985, 'Venus Northern Hemisphere: The Main Types of Structures', *Solar System Res.* **19**, 1–9.

Barsukov, V. L. et. al.: 1985, 'The Geology and Geomorphology of the Venus Surface as Revealed by the Radar Images Obtained by Venera 15 and 16', *J. Geophys. Res.* **91**, D378–D398.

Basilevsky, A. T.: 1993, 'Age of Rifting and Associated Volcanism in Atla, Regio, Venus', *Geophys. Res. Lett.* **20**, 883–886.

Basilevsky, A. T.: 1995, 'Coronae of Venus: A Stratigraphic Analysis of the Magellan Imagery', *Annale Geophysique, Part III, Space and Planetary Science* (Supplement III) **12**, C652.

Basilevsky, A. T.: 1996a, Geologic mapping of V17 Beta Regio Quadrangle: Preliminary Results', *Lunar Planet. Sci.* **27**, 65–66.

Basilevsky, A. T.: 1996b, 'On the Stratigraphic Significance of Wrinkle Ridges on Venus', *Lunar Planet. Sci.* **27**, 67–68.

Basilevsky, A. T.: 1997, 'Venera 8 Landing Site Geology Revisited', *J. Geophys. Res.* **102**, 9257–9262.

Basilevsky A. T. and Head J. W.: 1994, *Characteristics of the Geology of Thirty-six Sites on Venus*, Brown University Library, Providence RI, 72 pp.

Basilevsky, A. T. and Head, J. W.: 1995a, 'Global Stratigraphy of Venus: Analysis of a Random Sample of Thirty-six Test Areas', *Earth, Moon and Planets* **66**, 285–336.

Basilevsky, A. T. and Head, J. W.: 1995b, 'Regional and Global Stratigraphy of Venus: A Preliminary Assessment and Implications for the Geologic History of Venus, *Planet. Space Sci.* **43**, 1523–1553.

Basilevsky, A. T. and Head, J. W.: 1995c, 'Geologic History of Venus for the Last 300–500 m.y. Based on Photogeologic Analysis of the Magellan Images', *Astronomichesky Vestnik* **29**(3), 195–218 (in Russian).

Basilevsky, A. T. and Head, J. W.: 1996a, 'Evidence for Rapid and Widespread Emplacement of Volcanic Plains on Venus: Stratigraphic Studies in the Baltis Vallis Region', *Geophys. Res. Lett.* **23**, 1497–1500.

Basilevsky, A. T. and Head, J. W.: 1996b, 'Venus: Crater Chronology Overview and Geophysical Implications', *Lunar Planet. Sci.* **27**, 71–72.

Basilevsky, A. T., et al.: 1986, 'Styles of Tectonic Deformations on Venus: Analysis of Venera 15 and 16 Data', *J. Geophys. Res.* **91**, D399–D411.

Basilevsky, A. T., Nikolaeva, O. V., and Weitz, C. M.: 1992, 'Geology of the Venera 8 Landing Site Region from Magellan Data', *J. Geophys. Res.* **97**, 16315–16335.

Basilevsky, A. T., Head, J. W., Schaber, G. G., and Strom, R. G.: 1997a, 'The Resurfacing History of Venus', in S..W. Bougher, D. M. Hunten, and R. J. Phillips (Eds.), *Venus II – Geology, Geophysics, Atmosphere, and Solar Wind Environment*, University of Arizona Press, Tucson, pp. 1047–1086.

Basilevsky, A. T., Burba, G. A., Ivanov, M. A., Kryuchkov, V. P., Pronin, A. A., Bobina, N. N., Shashkina, V. P., and Head, J. W.,: 1997b, 'The Photogeologic Mapping of Northern Venus', *Lunar Planet. Sci.* **28**, 75–76.

Brewer, T. S., Hergt, J. M., Hawkesworth, C. J., Rex, D., and Storey, B. C.: 1992, 'Coats Land Dolerites and the Generation of Antarctic Continental Flood Basalts', in B. C. Storey, T. Alabaster, and R. J. Pankhurst (Eds.), *Magmatism and the Causes of Continental Break-up*, pp.185–208, *Geol. Soc. Spec. Pub.* **68**.

Bulmer, M. M.: 1996, 'An Examination of the Transport and Emplacement of Long Run-out Debris Masses Associated with Modified Domes on Venus, *Lunar Planet. Sci.* **27**.

BVSP (Basaltic Volcanism Study Project): 1981, *Basaltic Volcanism on the Terrestrial Planets*, Pergamon Press, New York, 1286 pp.

Campbell, D. B., Stacy, N. J. S., Newman, W. I. et al.: 1992, 'Magellan Observations of Extended Impact Crater Related Features on the Surface of Venus', *J. Geophys. Res.* **97**, 16249–16277.

Carr, M. H.: 1973, 'The Role of Lava Erosion In the Formation of Lunar Rilles and Martian Channels', *Icarus* **22**, 1–23.

Chapman, M. G. and Kirk, R. L.: 1996, 'A Migratory Mantle Plume on Venus: Implication for Earth?', *J. Geophys. Res.* **101**, 15,953–15,967.

Collins, G. C., Head, J. W., Ivanov, M. A., and Basilevsky, A.T.: 1997, 'Time Scale of Regional Plains Emplacement on Venus', *Lunar Planet. Sci.* **27**, 243–244.

Condie, C. C.: 1989, *Plate Tectonics and Crustal Evolution*, 3rd edition, Pergamon Press, New York, 476 pp.

Copp, D. L. and Guest, J. E.: 1995, 'Geology of the V31 Sif and Gula Quadrangle of Venus', *Lunar Planet. Sci.* **26**, 283–284.

Gilmore, M., Ivanov, M. A., Head, J. W., and Basilevsky, A. T.: 1997, 'Duration of Tessera Deformation on Venus', *J. Geophys. Res.* **102**, 13357–13368.

Griffiths, R. W. and Campbell, L. H.: 1991, 'Interaction of Mantle Plume Heads with the Earth's Surface and Onset on Small-Scale Convection', *J. Geophys. Res.* **96**, 18,295–18,310.

Head, J. W. and Ivanov, M. A.: 1996, 'Evidence for Regional Basin Formation In Early Post-Tessera Venus History: Geology of the Lavinia Planitia Area (VSS)', *Lunar Planet. Sci.* **27**, 515–516.

Head, J. W. and Wilson, L,: 1992, 'Lunar Mare Volcanism: Stratigraphy, Eruption Conditions, and the Evolution of Secondary Crusts', *Geochim. et Cosmochim. Acta* **56**, 2155–2175.

Head, J. W., Crumpler, L., Aubele, L., Guest, J., and Saunders, R. S.: 1992, 'Venus Volcanism: Classification of Volcanic Features and Structures, Associations, and Global Distribution from Magellan Data', *J. Geophys. Res.* **97**, 13,153–13,197.

Head, J. W., Parmentier, E. M., and Hess, P. C.: 1994, 'Venus: Vertical Accretion of Crust and Depleted Mantle and Implications for Geological History and Processes', *Planet. Space Sci.* **42**, 803–811.

Hess, P. C.: 1989, *Origin of Igneous Rocks*, Harvard University Press, Cambridge, 336 pp.

Hill, R. I., Campbell, I. H., Davies, G. F., and Griffiths, R. W.: 1992, 'Mantle Plumes and Continental Tectonics', *Science* **256**, 186–193.

Ivanov, M. A.: 1993, 'Geology of the Alpha Regio Vicinities on Venus Based on the Magellan Data', *Astronomichesky Vestnik* **27**(1), 3–18 (in Russian).

Ivanov, M. A. and Basilevsky, A. T.: 'Density and Morphology of Impact Craters on Tessera Terrain, Venus', *Geophys. Res. Lett.* **20**, 2579–2582.

Ivanov, M. A. and Head, J. W.: 1996, 'Tessera Terrain on Venus: A Survey of the Global Distribution, Characteristics, and Relation to Surrounding Units from Magellan Data', *J. Geophys. Res.* **101**, 14,861–14,908.

Ivanov, M. A. and Head, J. W.: 1997a, 'Venus: Stratigraphic Relationships and Geologic History in a Latitude Band at 30°N Latitude', *Brown-Vernadsky Microsymposium* **25**, Houston.

Ivanov, M. A. and Head, J. W.: 1997b, 'Stratigraphy of Venus Coronae in a Global Belt at 35 Degrees North', *26th International Symposium on Planetology*, Vernadsky/Brown, Moscow, pp. 30–31.

Jackson, E., Brown, D., and Grimm, R.: 1995, 'Rifting and Corona Formation in Eastern Aphrodite Terra, Venus', *Lunar Planet. Sci.* **26**, 665-666.

Jackson, E., Kryuchkov, V. P., and Pronin, A. A.: 1996, 'Geology of Bell Regio, Venus: A Stratigraphic Analysis with Special Reference to Assumptions', *Vernadsky-Brown Microsymposium* **24**, 136–27.

Janes, D. M. et al.: 1992, 'Geophysical Models for the Formation and Evolution of Coronae on Venus', *J. Geophys. Res.* **97**, 16,055–16,084.

Janes, D. M. and Squyres, S. W.: 1995, 'Viscoelastic Relaxation of Topographic Highs on Venus to Produce Coronae', *J. Geophys. Res.* **100**(E10), 21,173–21,187.

Kargel, J. S., Kirk, R. L., Fegley, B., and Treiman, A. M.: 1994, 'Carbonate-Sulfate Volcanism on Venus?', *Icarus*, **112**, 219–252.

Koch, D. M.: 1994, 'A Spreading Drop Model for Plumes on Venus', *J. Geophys. Res.* **99**, 2035–2052.

Kryuchkov, V. P.: 1996, 'Problems of Venus Stratigraphy Revealed in the Process of 1 : 10M Photogeologic Mapping of the Area between Ananke Tessera and Lakshmi Planum, Venus', *Lunar Planet Sci.* **27**, 713–714.

Magee, K. and Head, J. W.: 1993, 'Large-Scale Volcanism Associated with Coronae on Venus: Implications for Formation and Evolution', *Geophys. Res. Lett.* **20**, 1111–1114.

Magee, K. P. and Head, J. W.: 1995, 'The Role of Rifting in the Generation of Melt: Implications for the Origin and Evolution of the Lada Terra-Lavinia Planitia Region of Venus, *J. Geophys. Res.* **100**, 1527–1552.

Musser, G. S. and Squyres, S. W.: 1997, 'A Coupled Thermal-Mechanical Model for Corona Formation on Venus', *J. Geophys. Res.* **102**, 6581–6596.

Namiki, N. and Solomon, S. C.: 1994, 'Impact Crater Densities on Volcanoes and Coronae on Venus: Implications for Volcanic Resurfacing', *Science* **265**, 929–933.

Nikishin, A. M., Pronin, A. A., and Basilevsky, A. T.: 1992, 'Hot Spot Structures', in: V. L. Barsukov, A. T. Basilevsky, V. P. Volkov, and V. N. Zharkov (Eds.), *Venus Geology, Geochemistry and Geophysics*, University of Arizona Press, Tucson, pp. 31–67.

Parmentier, E. M. and Hess, P. C.: 1992, 'Chemical Differentiation of a Convecting Planetary Interior: Consequences for a One Plate Planet such as Venus', *Geophys. Res. Lett.* **19**, 2015–2018.

Pavri, B., Head, J. W., Klose, K. B., and Wilson, L.: 1992, 'Steep-Sided Domes on Venus: Characteristics, Geologic Setting, and Eruption Conditions from Magellan Data', *J. Geophys. Res.* **97**, 13,465–13,478.

Phillips, R. J., Raubertas, R. F. Arvidson, R. E., Sarkar, I. C., Herrick, R. R., Izenberg, N., and Grimm, R. E.: 1992, 'Impact Craters and Venus Resurfacing History', *J. Geophys. Res.* **97**(E10), 15,923–15,948.

Plaut, J. J., 1996, 'Geologic Map of Navka Planitia Quadrangle, Venus', *Lunar Planet. Sci.* **27**, 1039–1040.

Price, M. and Suppe, J.: 1994, 'Young Volcanism and Rifting on Venus', *Nature* **372**, 756–759.
Pronin, A. A.: 1997, 'Stratigraphic Position of Some Coronae on Venus', *Solar System Res.* **31**, 1–18.
Pronin, A. A. and Stofan, E. R.: 'Coronae on Venus: Morphology and Origin', *Lunar Planet. Sci.* **19**, 953–954.
Pronin, A. A. and Stofan, E. R.: 1990, 'Coronae on Venus: Classification and Distribution', *Icarus* **87**, 452–474.
Sandwell, D. T. and Schubert, G.: 'Flexural Ridges, Trenches, and Outer Rises Around Coronae on Venus', *J. Geophys. Res.* **97**, 16,069–16,084.
Saunders, R. S.: 1996, 'Venus Ovda Regio Stratigraphy and Tectonics: Highland-Plains Relationships', *Lunar Planet. Sci.* **27**, 1131–1132.
Schaber, G. G.: 1973, 'Lava Flows in Mare Imbrium: Geological Evaluation from Apollo Orbital Photography', *Proc. Lunar Sci. Conf 4th*, 73–92.
Schaber, G. G., Strom, R. G., Moore, H. J., Soderblom, L. A., Kirk, R. L., Chadwick, D. J., Dawson, D. D., Gaddis, L. R., Boyce, J. M., and Russell, J.: 1992, 'Geology and Distribution of Impact Craters on Venus: What are they Telling Us?', *J. Geophys. Res.* **97**(E8), 13,257–13,301.
Schubert, G., Bercovici, D., Thomas, R., and Campbell, D.: 1989, 'Venus Coronae: Formation by Mantle Plumes', *Lunar Planet. Sci.* **20**, 968–969.
Senske, D. A.: 1996, 'Geologic Mapping on the Juno Dorsum Quadrangle (V-47), Venus', *Lunar Planet. Sci.* **27**, 1171–1172.
Senske, D. A., Saunders, R. S., Stofan, E. R., and member of the Magellan Science Team: 1994, 'The Global Geology of Venus: Classification of Landforms and Geologic History', *Lunar Planet. Sci.* **25**, 1245–1246.
Smrekar, S. E. and Parmentier, E. M.: 1996, 'The Interaction of Mantle Plumes with Surface Thermal and Chemical Boundary Layers: Application to Hot Spots on Venus', *J. Geophys. Res.* **101**(B3), 5397–5410.
Smrekar, S. E. and Stofan, E. R.: 1996, 'Towards a Comprehensive Model of Coronae Formation on Venus', *Lunar Planet. Sci. 27th*, 1227–1228.
Solomon, S. C., Smrekar, S. E., Bindschadler, D. L., Grimm, R. E., Kaula, W. M., McGill, G. E., Phillips, R. J., Saunders, R. S., Schubert, G., Squyres, S. W., and Stofan, E. R.: 1992, 'Venus Tectonics: An Overview of Magellan Observations', *J. Geophys. Res.* **94**(E8), 13,199–13,256.
Squyres, S. W., et al.: 1992, 'The Morphology and Evolution of Coronae on Venus', *J. Geophys. Res.* **97**, 12,611–13,634.
Stofan, E. R. and Guest, J. E.: 1996, 'Geology of the Aino Planitia Quadrangle (V46): Relative Timing of Tectonism and Volcanism', *Lunar Planet. Sci.* **27**, 1277–1278.
Stofan, E. R. and Head, J. W.: 1990, 'Coronae of Memnosyne Regio, Venus: Morphology and Origin', *Icarus* **83**, 216–243.
Stofan, E. R. et al.: 1992, 'Global Distribution and Characteristics of Coronae and Related Features on Venus: Implications for Origin and Relation to Mantle Processes', *J. Geophys. Res.* **97**, 13,347–13,378.
Strom, R. G.: Parabolic Features and the Erosion Rate on Venus', *Lunar Planet. Sci.* **24**, 1371–1372.
Strom, R. G., Schaber, G. G., and Dawson, D. D.: The Global Resurfacing of Venus', *J. Geophys. Res.* **99**, 12,899–10,926.
Tanaka, K. L., Scott, D. H., and Greeley, R.: 1992, in: H. H. Kieffer, B. M. Jakosky, C. W. Snyder, and M. S. Matthews (Eds.), *Global Stratigraphy, in Mars*, University of Arizona Press, Tucson, pp. 345–382.
Tanaka, K. L., Senske, D. A., Price, M., and Kirk, R. L.: 1997, 'Physiography Geomorphic/Geologic Mapping and Stratigraphy of Venus, in: S. W. Bougher, D. M. Hunten, and R. J. Phillips (Eds.), *Venus II – Geology, Geophysics, Atmosphere, and Solar Wind Environment*, University of Arizona Press, Tucson, pp. 667–696.

Tolan, T. L., Reidel, S. D., Beeson, M. H., Anderson, J. L., Fecht, K. R., and Swanson, D. A.: 1989, 'Revision to the Estimates of the Areal Extent and Volume of the Columbia River Basalt Group', *Gel. Soc. Amer. Spec. Pap.* **239**, 1–20.

Wilhelms, D. E.: 1987, 'The Geologic History of the Moon', *U.S. Geol. Surv. Prof Pap.* **1348**.

Zahnle, K. and McKinnon, W.: 1996, 'Age of the Surface of Venus', *Bull. Amer. Astron. Soc.* **28**, 1119.